AD_____

Award Number:W81XWH-04-1-0810

TITLE: Origin of Prostate Cancer-associated Stroma: Epithelial Mesenchymal Transition (EMT)

PRINCIPAL INVESTIGATOR: Donna M. Peehl, Ph.D.

CONTRACTING ORGANIZATION: Stanford University
Stanford, CA 94305

REPORT DATE: March 2006

TYPE OF REPORT: Final

PREPARED FOR: U.S. Army Medical Research and Materiel Command
Fort Detrick, Maryland 21702-5012

REPORT DOCUMENTATION PAGE

Form Approved
OMB No. 0704-0188

1. REPORT DATE	2. REPORT TYPE	3. DATES COVERED
01-03-2006	Final	31 Aug 2004 – 28 Feb 2006

4. TITLE AND SUBTITLE

Origin of Prostate Cancer-associated Stroma: Epithelial Mesenchymal Transition (EMT)

5a. CONTRACT NUMBER

5b. GRANT NUMBER
W81XWH-04-1-0810

5c. PROGRAM ELEMENT NUMBER

6. AUTHOR(S)

Donna M. Peehl, Ph.D.

5d. PROJECT NUMBER

5e. TASK NUMBER

5f. WORK UNIT NUMBER

7. PERFORMING ORGANIZATION NAME(S) AND ADDRESS(ES)

Stanford University
Stanford, CA 94305

8. PERFORMING ORGANIZATION REPORT NUMBER

9. SPONSORING / MONITORING AGENCY NAME(S) AND ADDRESS(ES)
U.S. Army Medical Research and Materiel Command
Fort Detrick, Maryland 21702-5012

10. SPONSOR/MONITOR'S ACRONYM(S)

11. SPONSOR/MONITOR'S REPORT NUMBER(S)

12. DISTRIBUTION / AVAILABILITY STATEMENT
Approved for Public Release; Distribution Unlimited

13. SUPPLEMENTARY NOTES
Original contains colored plates: ALL DTIC reproductions will be in black and white.

14. ABSTRACT
Our objective was to explore the hypothesis that prostate cancer-associated stromal cells are derived from malignant epithelium by the process referred to as epithelial-mesenchymal transition (EMT). The first aim was to try to generate fibroblasts from primary cultures of prostate cancer cells. Despite trying several approaches, including treatment with a classic inducer of EMT, transforming growth factor (TGF), we saw no evidence of generation of fibroblasts. Aim 2 was to search for evidence of EMT in prostate cancer stroma, and here also we saw no evidence of EMT. Finally, our 3rd aim was to determine whether the properties of cancer-derived stromal cells are consistent with their origin by EMT. We performed cDNA microarray analyses to accomplish this aim and identified expression of particular genes whose activities may be related to EMT. Overall, our results do not strongly support the hypothesis that prostate cancer stroma arises from the malignant epithelium by EMT. However, alternative explanations for our lack of supporting evidence can be put forth that suggest future studies to continue to explore this hypothesis.

15. SUBJECT TERMS
prostate cancer stroma, epithelial mesenchymal transition, Stromal-epithelial interactions

16. SECURITY CLASSIFICATION OF:				18. NUMBER OF PAGES	19a. NAME OF RESPONSIBLE PERSON
a. REPORT	b. ABSTRACT	c. THIS PAGE			USAMRMC
U	U	U	UU	95	19b. TELEPHONE NUMBER *(include area code)*

Table of Contents

INTRODUCTION

The stroma of prostate cancer is deemed to be an important player in the malignant process, and recent studies have led to some new concepts about the nature of the cancer-associated stroma. The cancer stroma is now considered to be a "reactive" stroma, with features similar to those that occur during a generic wound response. The reactive stroma is believed to develop in response to paracrine signals from the malignant epithelium.

However, if the presence of a reactive stroma were due only to paracrine effects from the malignant epithelium, then the features of the reactive stroma would abate upon the absence of the malignant epithelium. This is not the case, because when cancer-associated stromal cells are placed into culture without malignant epithelial cells, they still retain distinctive features compared to stromal cells cultured from normal or benign tissues. For example, one of the striking features that distinguishes cancer-associated from normal stromal cells is their ability to make immortal but nontumorigenic prostatic epithelial cells tumorigenic. It is clear that at least some of the unique properties of the "reactive" stroma of cancer are not due solely to the environment but represent permanent alterations of the stromal cells themselves.

In this project, we proposed an alternate hypothesis to explain the nature of the "reactive" stroma in prostate cancer. We suggested that the unique properties of cancer-associated stroma are due to their origin from the malignant epithelium itself by a process known as epithelial-mesenchymal transition (EMT). This hypothesis was based on publications suggesting that EMT is responsible for the majority of new fibroblasts that are created during fibrosis associated with wounding or inflammation. In addition, there were publications suggesting that the stroma in breast cancer was derived by EMT. Furthermore, the recently reported EMT proteome was similar to that of the reactive stroma. The prototypic inducer of EMT, transforming growth factor (TGF)-β, is also implicated as a key inducer of the reactive stroma.

To test our hypothesis, we proposed three aims. The first was to see whether we could generate fibroblasts from primary cultures of human prostatic cancer cells by exposure to classic inducers of EMT. The second aim was to try to find evidence of EMT in the stroma of prostate cancer tissues. The third aim was to determine whether the properties of stromal cells cultured from prostate cancer are consistent with their origin by EMT.

BODY

Our first designated task was to see if fibroblasts could be generated from primary cultures of prostate cancer cells. For these studies, we used primary cultures of pure epithelial cells derived from cancers of several different individuals. First, we treated cancer cells with 1 ng/ml of TGFβ, a classic inducer of EMT, for up to one week. We had previously shown that TGFβ changes the morphology of these cells from epithelial-like (cuboidal) to fibroblast-like (elongated) [1], and we noted this same morphologic change in the treated cultures. Immunocytochemistry was used to assess the expression of the epithelial marker, keratin 18 (K18), and the fibroblastic marker of EMT, smooth muscle α-actin, in the treated cancer cell population. These experiments were done in such a way that even one cell in one million that

expressed smooth muscle α-actin would have been visible, but we saw no cells expressing this marker of EMT. The positive control, prostate smooth muscle cells, were stained with the antibody against smooth muscle α-actin, showing that the immunocytochemical procedure worked. In conjunction, all cancer cells maintained expression of the epithelial marker, K18.

We repeated this type of experiment in several different primary cultures, varying the conditions to see if smooth muscle α-actin – positive cells could be generated from the malignant epithelium. Among the parameters that were tested were cell density, since one report showed that EMT occurred most efficiently in sparse rather than dense cell cultures [2]. Another report showed that adding tumor necrosis factor (TNF)-α to TGFβ enhanced EMT [3], so we tested that combination of factors. None of these conditions resulted in generation of fibroblasts from cancer cells, as monitored by expression of the classic marker of EMT, smooth muscle α-actin. We concluded that we were unable to generate fibroblasts from prostate cancer cells, which did not support our hypothesis.

Our second aim was to demonstrate evidence of EMT in prostate cancer tissue. This aim turned out to be very technically challenging. Our goal was to look for keratin-positive cancer cells that also expressed the fibroblastic marker, FSP1, in tissues. We performed immunohistochemistry on formalin-fixed sections, focusing on grade 4 cancers. We could not identify any stromal cells that co-expressed keratin 18 and FSP1. This finding also did not lend support to our hypothesis.

Our third aim was to determine whether the properties of cultured cancer-associated stromal cells are consistent with their origin by EMT. To address this question, we undertook an extensive analysis of gene expression of stromal cells cultured from cancer versus benign tissues. The results were compiled in a manuscript submitted for publication and currently under revision for *Journal of Cellular Physiology*. This manuscript is included in the Appendix, so only the salient points will be reviewed here.

In our study, we profiled 18 stromal cell cultures [2 from normal transition zone, 4 from benign prostatic hyperplasia (BPH), 5 from cancer and 7 from normal peripheral zone] using cDNA microarrays. RNA was collected from quiescent cells in order to minimize variables associated with different rates of proliferation. SAM analysis identified genes that showed differential expression with statistical significance between the different types of stromal cells. Genes differently expressed between stromal cells from cancer versus normal peripheral zone are of most relevance here. We found 101 genes upregulated in cancer-derived stromal cells. Of these, autotaxin (ENPP2) was the gene most significantlyupregulated (7.4-fold higher in cancer-derived stromal cells compared to normal cells). While autotaxin is not a "classic" marker of EMT, autotaxin was one of the genes most highly upregulated in cyclosporine A-induced EMT of renal tubular cells (a model of renal fibrosis) [4]. Increased invasion and migration are associated with EMT, and autotaxin stimulates those activities. Our finding that autotaxin is significantly elevated in cancer-derived stromal cells is the only evidence we found in this study that tends to support our hypothesis.

In another study with a collaborator, Dr. Trevor Penning, we profiled transcripts of genes involved in androgen signaling in stromal cells derived from cancer versus normal or BPH. The

results from this study have been submitted for publication, and the manuscript is included in the Appendix. The genes investigated included those encoding enzymes that regulate levels of ligands for the androgen receptor (AR) or estrogen receptor (ER) [type 2 5α-reductase, aldo-keto reductases 1C1-1C4, retinol dehydrogenase-like 3α-hydroxysteroid (RL-HSD), 11-cis retinol dehydrogenase (RODH), L-3-hydroxyacyl coenzyme A dehydrogenase/type 10 17β-hydroxysteroid dehydrogenase (ERAB), novel type of human microsomal 3α-hydroxysteroid dehydrogenase, cytochrome P450 7B1] and nuclear receptors (AR, ER-α and -β). A significant increase in expression was observed in cancer-derived stromal cells compared to normal stromal cells for RODH4, RODH5, and ERAB. These enzymes have been implicated in the oxidation of 3α-diol back to dihydrotestosterone (DHT), which would potentially provide an increased growth stimulus through the AR to the malignant epithelium. The ratio between AR and ER was also different in cancer-derived versus normal stromal cells, with more AR relative to ER -α in the cancer-derived stromal cells. A decrease in the ratio of AKR1C1:AKR1C2 in cancer compared to normal stromal cells indicates that the 3β-diol signal will be reduced in the cancer stroma. Since 3β-diol is a pro-apoptotic ligand for ERβ, decreased 3β-diol in the cancer stroma would suggest loss of a growth restraint mechanism. Overall, these results suggest that alterations in the cancer-associated stroma in signaling pathways mediated by androgen and estrogen receptors might lead to greater growth stimuli of the malignant epithelium through paracrine signals. While these data do not directly relate to EMT, they do add additional information regarding abnormalities in cancer-associated stroma that could promote tumor growth.

KEY RESEARCH ACCOMPLISHMENTS

- Attempted to induce EMT in primary cultures of prostatic cancer cells by several methods but found no evidence of generation of stromal cells from the malignant epithelium by EMT
- Searched for evidence of EMT in the stroma of prostate cancer tissues but found no stromal cells expressing both epithelial and stromal markers simultaneously
- Carried out genetic profiling of stromal cells cultured from cancer and normal prostatic tissues and found that autotaxin, associated with EMT, was significantly higher in cancer stromal cells

REPORTABLE OUTCOMES

Zhao, H., Ramos, C.F., Brooks, J.D. and Peehl, D.M. Distinctive gene expression of prostatic stromal cells cultured from diseased versus normal tissues. Submitted to J. Cell. Physiol., under revision.

Bauman, D.R., Steckelbroeck, S., Peehl, D.M. and Penning, T.M. Transcript profiling of the androgen signal in normal prostate, benign prostatic hyperplasia and prostate cancer. Submitted to Cancer Res., under review.

CONCLUSIONS

During the course of our project, whether EMT is a real process and actually occurs in human cancers has become a subject of great debate [5,6]. Our results do not lend support to our hypothesis, which was that the cancer-associated stroma is derived from the malignant prostatic epithelium by the process of EMT. However, there may be technical or other reasons for our generally negative results. For example, our inability to convert primary cultures of cancer cells to fibroblasts does not add support to our hypothesis, but on the other hand, it does not completely negate the possibility. We might modify the hypothesis by suggesting that EMT is a property only of cancer stem cells, but not of the malignant epithelium as a whole. For a variety of reasons, we do not believe that our primary cultures of cancer cells contain stem cells. As stem cell research progresses, we will be able to test our hypothesis again, but by treating cancer stem cells instead of standard primary cultures with classic inducers of EMT. Similarly, our inability to detect cells in the stroma of cancer tissues that simultaneously expressed both epithelial and stromal markers (i.e., a cell in the process of undergoing EMT) may be due to the technical challenge of detecting these presumably rare cells. Finally, our genetic profiling studies revealed additional differences between cancer-derived and normal stromal cells that may or may not be related to EMT. The gene most highly overexpressed in cancer-derived stromal cells, autotaxin, has been associated with EMT. Autotaxin increases invasion and migration, classic behavior associated with EMT. Overall, our results do not definitively rule out or support our hypothesis, and additional studies are required.

REFERENCES

1. Peehl, D.M., Wong, S.T., Bazinet, M. and Stamey, T.A. *In vitro* studies of human prostatic epithelial cells: attempts to identify distinguishing features of malignant cells. Growth Factors 1:237-250, 1989.

2. Masszi, A., Fan, L., Rosivall, L., McCulloch, C.A., Rotstein, O.D., Mucsi, I. and Kapus, A. Integrity of cell-cell contacts is a critical regulator of TGF-β1-induced epithelial-to-myofibroblast transition. Am. J. Pathol. 165:1955-1967, 2004.

3. Willis, B.C., Liebler, J.M., Luby-Phelps, K., Nicholson, A.G., Crandall, E.D., du Bois, R.M. and Borok, Z. Induction of epithelial-mesenchymal transition in alveolar epithelial cells by transforming growth factor-β1. Am. J. Pathol. 166:1321-1332, 2005.

4. Slattery, C., Campbell, E., McMorrow, T. and Ryan, M.P. Cyclosporin A-induced renal fibrosis: a role for epithelial-mesenchymal transition. Am. J. Pathol. 167:395-407, 2005.

5. Tarin, D**.** The fallacy of epithelial mesenchymal transition in neoplasia. Cancer Res. 65: 5996-6001, 2005.

6. Cardiff, R.D. Epithelial to mesenchymal transition tumors: fallacious or snail's pace? Clin. Cancer Res. 11:8534-8537, 2005.

APPENDICES

Manuscript: Zhao, H., Ramos, C.F., Brooks, J.D. and Peehl, D.M. Distinctive gene expression of prostatic stromal cells cultured from diseased versus normal tissues. Submitted to J. Cell. Physiol., under revision.

Manuscript: Bauman, D.R., Steckelbroeck, S., Peehl, D.M. and Penning, T.M. Transcript profiling of the androgen signal in normal prostate, benign prostatic hyperplasia and prostate cancer. Submitted to Cancer Res., under review.

Distinctive gene expression of prostatic stromal cells cultured from diseased versus normal tissues

Hongjuan Zhao[1], Cristiane F. Ramos[2], James D. Brooks[1], and Donna M. Peehl[1]*

[1]Department of Urology, Stanford University, Stanford, California; [2]Urogenital Research Unit, State University of Rio de Janeiro, Brazil

Correspondence to: Donna Peehl, Department of Urology, Stanford Medical Center, Stanford, CA 94305-5118. Tel: 650-725-5531; Fax: 650-723-4200; Email: dpeehl@stanford.edu

Running head: Gene expression in prostatic stromal cells

Keywords: gene expression profiling, prostatic stromal cells, benign prostatic hyperplasia, prostate cancer

The total number of figures is five and the total number of tables is five.

Funded by: Department of defense; Grant number: W81XWH-04-1-0810.

Abstract

To obtain a comprehensive view of the transcriptional programs in prostatic stromal cells of different histological/pathological origin, we profiled 18 adult human stromal cell cultures from normal transition zone (TZ), normal peripheral zone (PZ), benign prostatic hyperplasia (BPH), and prostate cancer (PCA) using cDNA microarrays. A hierarchical clustering analysis of 714 named unique genes whose expression varied at least threefold from the overall mean abundance in at least three samples in all 18 samples demonstrated that cells of different origin displayed distinct gene expression profiles. Many of the differentially expressed genes are involved in biological processes known to be important in the development of prostatic diseases including regulation of cell proliferation and apoptosis, cell adhesion, and immune response. SAM analysis identified genes that showed differential expression with statistical significance including 24 genes between cells from TZ vs. BPH, 34 between BPH vs. PCA, and 101 between PZ vs. PCA. S100A4 and SULF1, the most up- and down-regulated gene in BPH vs. TZ, respectively, showed expression at the protein level consistent with microarray analysis. In addition, sulfatase assay showed that BPH cells have lower SULF1 activity compared to TZ cells. Quantitative real time polymerase chain reaction (PCR) analysis confirmed differential expression of ENPP2/autotaxin and OGN between PZ vs. CA, as well as differential expression of six genes between BPH vs. CA. Our results support the hypothesis that prostatic stromal cells of different origin have unique transcriptional programs and point towards genes involved in actions of stromal cells in BPH and PCA.

Introduction

Stromal cells of the prostate are known to regulate epithelial growth as well as support and maintain epithelial function. Classic rodent studies have shown that stroma is a major inducer of epithelial cell growth and differentiation in prostate development by mediating androgen actions (Cunha, 1984; Cunha et al., 1987). These experiments demonstrated that prostatic development only occurrs when embryonic stroma (UGM, an androgen receptor-positive, mesodermally-derived tissue) and epithelium (UGE, an endodermally-derived tissue) are recombined before implantation under the renal capsule of experimental animals, but not when implanted separately (Chung and Cunha, 1983; Cunha et al., 1983b). In addition, while wild type UGM can induce urinary bladder epithelium to undergo a complete redifferentiation to a prostatic phenotype, androgen-insensitive UGM (which lacks the androgen receptor) fail to induce prostatic differentiation of UGE (Cunha et al., 1983a; Cunha et al., 1980).

The stroma also plays an important role in the pathogenesis of prostate diseases (Chung et al., 2005; Cunha et al., 2002; Lee and Peehl, 2004). For instance, the earliest manifestation of benign prostatic hyperplasia (BPH) is the appearance of the mesenchyme in periurethral nodules, which has similar morphology to the prostatic mesenchyme during embryogenesis (McNeal, 1978). In later stages of BPH development, glandular budding and branching toward a central focus leads to further nodule growth (McNeal, 1978). Such morphological evidence suggests that BPH is intrinsically a mesenchymal disease that results from a reawakening of embryonic inductive interactions between the prostatic stroma and epithelium. In prostate cancer, the stroma generated by the recruiting signals released from adenocarcinoma cells,

called “reactive stroma”, is similar to the stroma at the sites of wound repair both histologically and molecularly (Chang et al., 2004; Condon, 2005; Tuxhorn et al., 2001). Reactive stroma from prostate cancer has been shown to stimulate cancer cell growth and migration and to promote angiogenesis by altering the balance of angiogenesis activators and inhibitors (Tuxhorn et al., 2002a; Tuxhorn et al., 2002b). In addition, reactive stroma has been associated with the clinical course of prostate cancer, with increased reactive stroma predicting progression and worse outcome (Ayala et al., 2003). Finally, reactive stroma is capable of transforming a non-tumorigenic prostatic epithelial cell line (BPH-1) to a malignant one (Hayward et al., 2001). It becomes clear that the stroma in prostate cancer not only provides a supportive microenvironment that promotes tumor progression, but also is a critical determinant of benign versus malignant growth.

Despite the importance of stromal cells in prostate development, function and disease, a comprehensive view of the transcriptional programs in stromal cells of different histological and pathological origin is currently lacking. Such information may provide not only new insights into the biology of prostate pathogenesis, but also novel therapeutic strategies aimed at preventing the generation of stroma important for disease development and progression. For instance, genes comprising a stereotypical gene expression program in response to serum exposure by fibroblasts from ten different anatomic sites have been shown to be coordinately regulated in many human tumors including prostate cancer (Chang et al., 2004). This transcriptional signature of the response of fibroblasts to serum has also been shown to be a powerful predictor of the clinical course in several common carcinomas.

Although prostatic stromal cells cultured from different histological and pathological origins are similar in certain phenotypic features including their morphology, population doubling time, cell cycle distribution and response to genotoxic and chemotoxic agents, they differ in a number of aspects (San Francisco et al., 2004). First, carcinoma-associated fibroblasts (CAF) exhibit an increased potential to undergo anchorage-independent growth in soft agar compared to fibroblasts cultured from normal human prostate (NHPF) (San Francisco et al., 2004). Second, stromal cells from BPH (BPHF) and cancer tissues show different capability in inducing the growth of BPH-1 epithelial cells in tissue recombinant experiments (Barclay et al., 2005). BPH-1 recombinants with BPHF produced small grafts with similar histology to BPH. In contrast, CAF produced aggressive prostatic tumors when recombined with BPH-1 cells (Barclay et al., 2005). Finally, a number of molecules have been shown to be differentially expressed by stromal cells of different histology or pathology. For example, transforming growth factor $(TGF)_{\beta}$-1 is expressed in higher concentrations in CAF than NHPF, which may contribute to the higher capability of CAF to form colonies in soft agar and the ability of CAF to promote malignant progression of prostate epithelial cells (San Francisco et al., 2004). In addition, a number of growth factors and cytokines are reportedly overexpressed in BPH stroma including fibroblast growth factor (FGF)-2, FGF-7, insulin-like growth factor (IGF)-1, IGF-2, and interleukin (IL)-1α (Lee and Peehl, 2004). Based on these observations, we hypothesize that prostatic stromal cells of different histological and pathological origins have distinct transcriptional programs. To test this hypothesis, we profiled 18 human stromal cell cultures from normal transition zone (TZ), normal peripheral zone (PZ), BPH, and cancer (CA) tissues using cDNA microarrays containing 24,473 unique genes. We compared gene expression profiles of BPH cells to normal TZ cells because the TZ is the main site of origin of BPH. Similarly, we compared gene expression profiles of CA cells to normal PZ cells because the majority of prostate cancer arises in the PZ.

Material and Methods

Cell culture

Primary cultures of human prostatic stromal cells were established from histologically confirmed normal, BPH, or CA tissues according to previously described methods (Peehl and Sellers, 2000). The primary cell cultures used in this study are listed in Table 1. The presence of contaminating epithelial cells was ruled out by the absence of staining with antibodies against epithelial keratins 5 and 18 (Enzo Life Sciences, Inc., Farmingdale, NY). These cultures were serially passaged in SCGM™ (Cambrex, East Rutherford, NJ) supplemented with 5 µg/ml insulin, 1 ng/ml FGF-2, 5% fetal bovine serum (FBS) and 100 µg/ml of gentamycin. At passages 8 to 19, cells were seeded on 100-mm cell culture dishes with 1 million cells/dish. Twenty four hours later, cells were switched to MCDB 105 (Sigma-Aldrich, St. Louis, MO) with 100 µg/ml of gentamycin. Total RNA was isolated another 24 hours later. MCF-7 cells were cultured in DMEM (Invitrogen™, Carlsbad, CA) supplemented with 10% FBS and MCF-10A cells were cultured in DMEM/F12 (Invitrogen™) supplemented with 15 mM HEPES buffer, 5% horse serum, 10 µg/ml insulin, 20 ng/ml epidermal growth factor (EGF), 100 ng/ml cholera toxin, and 0.5 µg/ml hydrocortisone.

RNA isolation and microarray hybridization

Total RNA was isolated using TRIzol solution (Invitrogen™) according to manufacturer's instructions. Fluorescently-labeled DNA probes were prepared from 50 to 70 µg total RNA isolated from prostatic stromal cells (Cy5-labeled) and Universal Human Reference RNA (Stratagene, La Jolla, CA) (Cy3-labeled) by reverse transcription using an Oligo dT

primer 50- TTTTTTTTTTTTTTT-30 (Qiagen, Valencia, CA) as described previously (Zhao et al., 2005). Labeled probes from each stromal cell RNA and reference RNA were mixed and hybridized overnight at 65°C to spotted cDNA microarrays with 41,126 elements (Stanford Functional Genomics Facility, Stanford, CA). Microarray slides were then washed to remove unbound probe and scanned with a GenePix 4000B scanner (Axon Instruments, Inc., Union City, CA).

Data processing and analysis

The acquired fluorescence intensities for each fluoroprobe were analyzed with GenePix Pro 5.0 software (Axon Instruments, Inc.). Spots of poor quality were removed from further analysis by visual inspection. Data files containing fluorescence ratios were entered into the Stanford Microarray Database (SMD) where biological data were associated with fluorescence ratios and genes were selected for further analysis (Sherlock et al., 2001). Hierarchical clustering was performed by first retrieving only spots with a signal intensity >150% above background in either Cy5- or Cy3-channels in at least 70% of the microarray experiments from SMD. We selected clones whose expression levels varied at least three-fold in at least three of the samples from the mean abundance across all samples. The genes and arrays in the resulting data tables were ordered by their patterns of gene expression using hierarchical clustering analysis, and visualized using Treeview software (http://rana.lbl.gov/EisenSoftware.htm). Genes with potentially significant differential expression in stromal cells from different histological/pathological origins were identified using the Significance Analysis of Microarrays (SAM) procedure, which computes a two-sample T-statistic (e.g., for BPH vs. TZ cells) for the normalized log ratios of gene expression levels for each gene (Tusher et al., 2001). The procedure thresholds the T-statistics to provide a 'significant' gene list and provides an estimate of the false-discovery rate (the percentage of genes

identified by chance alone). We used a selection threshold that gives a relatively low false discovery rate and identifies a relatively high number of significant genes.

Quantitative Real-Time PCR (qRT-PCR)

Total RNA from stromal cells was reverse transcribed as described above. cDNA product was then mixed with DyNAmo SYBR® Green master mix (Biolabs, Ipswich, MA) and primers of choice in the subsequent PCR reaction using a DNA Engine Opticon® 2 Continuous Fluorescence Detection System (MJ Research, Hercules, CA) according to manufacturer's instructions. Each reaction was done in triplicate to minimize the experimental variations (standard deviation was calculated for each reaction). Transcript levels of TATA box binding protein (TBP) were assayed simultaneously with each of the 29 genes selected for validation as an internal control to normalize their transcript levels. A list of the primer sequences used is available at http://genome-www5.stanford.edu/cgi-bin/tools/display/listMicroArrayData.pl?tableName=publication.

Immunochemistry

F-TZ-1 and F-BPH-4 cells cultured on 8-well chamber slides were fixed in 2% paraformaldehyde and permeabilized in 95% ice-cold ethanol. Horse serum [10% in phosphate-buffered saline (PBS)] was used to block non-specific binding of antibodies. The slide was then incubated at room temperature (RT) for 30 minutes in the primary antibody. A mouse monoclonal antibody against human SULF1 (CBI PGA antibody core, Tempe, Arizona) and a rabbit polyclonal antibody against S100A4 (Santa Cruz Biotechnology, Inc., Santa Cruz, CA) were used at a 1:50 dilution. The slides were then washed and incubated in a biotinylated secondary antibody at RT for 30 minutes, washed and incubated again at RT for another 30 minutes in peroxidase-conjugated

streptavidin. Color was developed with 3′,3′ diaminobenzidine (DAB) (DakoCytomation California Inc., Carpinteria, CA). Counter staining was performed with hematoxylin. A similar procedure was used for tissue sections, except that tissues were first deparaffinized in xylene, and hydrated in a graded series of alcohol. Slides were then incubated in 0.3% hydrogen peroxide in methanol for 15 min and 10% horse serum for 20 min at RT before incubation in the primary antibody at 4°C overnight.

Western Blotting

Cells were lysed with lysis buffer [pH 7.5, 50 mM HEPES, 0.5% NP-40, 0.25% Na-deoxycholate, 0.1 mM sodium vanadate, 50 mM NaCl, 1 mM EDTA, 1 mM phenylmethylsulfonyl fluoride (PMSF)]. Protein concentration was determined using the Bradford assay (Bio-Rad, Hercules, CA). Twenty micrograms of protein were separated using a 10% NuPAGE® 10% Bis-Tris Gel (Invitrogen) and transferred to a Hybond-P membrane (Amersham Life Sciences, Arlington Heights, IL). S100A4 was detected with a rabbit polyclonal anti-human antibody A5114 (DakoCytomation) and visualized with an ECL Plus kit (Amersham Biosciences, Piscataway, NJ). Glyceraldehyde-3-phosphate dehydrogenase (GAPDH) was detected with a monoclonal mouse anti-rabbit antibody, MoAb 6C5, which reacts with human GAPDH (Research Diagnostics, Flanders, NJ). S100A4 and GAPDH signal intensities were quantified with a Scion Image (http://www.meyerinst.com/html/scion/scion_image_windows.htm).

In situ hybridization

In situ hybridization of tissue sections was performed based on a protocol published previously (West et al., 2004). Briefly, digoxigenin (DIG)-labeled sense and anti-sense RNA probes were generated by in vitro transcription using templates produced by PCR amplification of a 498 bp product with the T7 promoter incorporated into the primers. In

vitro transcription was performed with a DIG RNA-labeling kit and T7 polymerase according to the manufacturer's protocol (Roche Diagnostics, Indianapolis, IN). Tissue sections of 5 μm thick from paraffin blocks were digested in 10 μg/ml of proteinase K at 37 ^{o}C for 30 minutes and hybridized overnight at 55 ^{o}C with either sense or anti-sense riboprobes at 200 ng/ml dilution in mRNA hybridization buffer (DAKO). The following day, sections were incubated with a 1:35 dilution of RNase A cocktail (Ambion, Austin, TX) for 30 minutes at 37 ^{o}C, followed by stringent washing. For signal amplification, a HRP-conjugated rabbit anti-DIG antibody (DAKO) was used to catalyze the deposition of biotinyl tyramide, followed by secondary streptavidin complex (GenPoint kit; DAKO). The final signal was developed with DAB (GenPoint kit; DAKO). For sense RNA probe, the primer sequences were 5'CTAATACGACTCACTATAGGGATACTCGGCAGACACGTTCC3' and 5'CCTCCTTGAATGGGTGAAGA3′. For anti-sense RNA probe, the primer sequences were 5'CTAATACGACTCACTATAGGGCCTCCTTGAATGGGTGAAGA3' and 5′ATACTCGGCAGACACGTTCC3′.

Sulfatase assay

F-TZ-1 or F-BPH-4 cells were cultured as described above and the assay was performed according to previously published protocols with modifications (Lai et al., 2004a). After 24 hrs in serum-free medium, cells were washed in ice-cold PBS and lysed in SIE buffer (250 mM sucrose, 3 mM imidazole, pH 7.4, 1% ethanol) containing 1% (w/v) Nonidet P-40 and 1 mM PMSF. Protein concentration was determined as described above. The total cellular protein (20 μg) was preincubated with 10 μM estrone-3-O-sulfamate (Sigma-Aldrich) at 37°C for 1 hr to inhibit steroid sulfatases. 4-methylumbelliferyl sulfate was then added to a final concentration of 7.5 mM in a total volume of 200 μl. After incubation for 24 hr at 37°C, the reaction was terminated by

addition of 1 ml of 0.5 M Na_2CO_3/$NaHCO_3$, pH 10.7. The fluorescence of the liberated 4-methylumbelliferone was measured using excitation and emission wavelengths of 355 and 460 nm, respectively. MCF-7 and MCF-10A cells were used as positive and negative controls, respectively. Each reaction was performed in triplicate and standard deviation was calculated. The enzymatic activities of SULF1 in MCF-7, F-TZ-1, and F-BPH-4 cells were normalized against that in MCF-10A.

Results

Gene expression profiles in prostatic stromal cells

We profiled gene expression of 18 stromal cell cultures including 4 from BPH, 2 from normal TZ, 5 from CA, and 7 from normal PZ (Table 1). In order to standardize culture conditions at the time of analysis, one million cells were inoculated into each of seven 100 mm dishes containing SCGM^{TM}. Twenty-four hours later, cells were changed to serum-free medium, then RNA was isolated 24 hours later. A hierarchical clustering analysis of 714 named unique genes represented by 1,032 clones whose expression varied at least threefold from the overall mean abundance in at least three samples in all 18 samples tested is shown in Figure 1A. In the dendrogram (Figure 1B), BPH stromal cells were separated from normal TZ stromal cells, demonstrating that prostate stromal cells from normal TZ and BPH tissues have distinct gene expression patterns. CA stromal cells were grouped in a tight cluster away from cells from other histological/pathological origins except for one PZ stromal cell culture, indicating a unique transcriptional program associated with cancer-derived stromal cells. Note that two duplicate hybridizations of F-CA-1 clustered next to each other, showing a high reproducibility of the method. Interestingly, the PZ cultures showed heterogeneity in their gene expression profiles, as they were broken into three groups by the clustering algorithm. F-PZ-1, -5, and –7 were similar to each other in their expression patterns, where as F-PZ-2, -3, and –4 were alike. F-PZ-6, on the other hand, showed a similar expression profile to CA cells for reasons other than misdiagnosis since the histology of the area of tissue where the cells came from was confirmed as normal. In addition, varying gene selection criteria didn't change the association of samples significantly (Figure 1C, 1D), suggesting a robust clustering. Of the named genes, more than 80% have some biological annotations associated according to Gene Ontology (GO). Many

of them are involved in biological processes that are known to be important in the development of prostatic diseases including regulation of cell proliferation and apoptosis, cell adhesion, and immune response. See http://genome-www5.stanford.edu/cgi-bin/tools/display/listMicroArrayData.pl?tableName=publication for a complete list of genes.

Identification of genes differentially expressed using SAM analysis

The SAM procedure was used to identify genes with statistically significant differences in expression between groups of samples, because SAM accurately identifies transcripts with reproducible changes in gene expression and is more reliable than conventional means of analyzing microarrays (Tusher et al., 2001). Three comparisons were made between stromal cells of different histological/pathological origins. First, gene expression of BPH cells was compared to that of cells from TZ, the zone of origin of BPH. Thirty-four clones representing 24 unique named genes were selected by SAM as differentially expressed between TZ and BPH cells with a false positive rate of 24%. Of these, 21 were overexpressed in BPH compared to TZ cells, whereas 3 were underexpressed. Except for 3 of these genes, the others have been characterized to different extents according to GO annotations. The average-fold differences in expression of these genes between BPH vs. TZ cells, ranks in SAM analysis, and GO annotations are listed in Table 2.

The next comparison was of genes expressed by stromal cells from the two different pathological diseases, BPH and cancer. Forty-eight clones representing 34 unique named genes were selected by SAM as differentially expressed between BPH and CA cells with a false positive rate of 13%. Of these, 28 were overexpressed in BPH cells compared to CA cells, whereas 6 were overexpressed in CA cells compared to BPH

cells. Thirty of the 34 genes have biological annotations in GO. The average- fold differences in expression of these genes between BPH vs. CA cells, ranks in SAM analysis, and GO annotations are listed in Table 3.

Finally, genes expressed by CAF were compared to those expressed by normal cells from the PZ, the major zone of origin of adenocarcinomas in the prostate. One hundred and seventeen clones representing 101 unique named genes were selected by SAM as differentially expressed between PZ and CA stromal cells with a false positive rate of 12%, all of which were overexpressed in CA compared to PZ cells. Sixty-eight genes that have biological annotations are listed in Table 4. The false positive rates of SAM analysis were relatively high, possibly due to the small sample sizes.

Validation of microarray data by qRT-PCR

To confirm the gene expression changes observed by microarray analysis, real-time RT-PCR was performed on selected genes identified by SAM analysis. We tested a total of 29 genes (14 for BPH vs. TZ, 7 for BPH vs. CA, and 8 for CA vs. PZ) using qRT-PCR, and determined the significance of differential expression by t-test (Table 5). Nine of 14 genes (64%) were validated for the BPH vs. TZ comparison, and 6 of 7 genes (86%) for BPH vs. CA. As an example, relative expression levels of SULF1 and S100A4, the most under- and over-expressed genes in BPH vs. TZ cells, respectively, are shown in Figure 2. Expression of the top most differentially expressed genes in CA cells vs. BPH cells, BST1 and OGN, were also confirmed (Figure 2). These results demonstrated that the gene expression differences in BPH vs. TZ and BPH vs. CA discovered by microarray analysis are reliable.

In comparison, only 2 of 8 genes (25%) were validated for PZ vs. CA (Table 5). There does not seem to be an association between SAM rank and the outcome of validation. Several possible reasons may underlie the low validation rate for the CA vs. PZ comparison. For instance, it could be that most of the genes we chose happen to be the ones that are not differentially expressed. In addition, the heterogeneity of gene expression among PZ cultures, and the differences in statistical methods (SAM vs. t-test) may also contribute to the observed differences in the results.

SULF1 and S100A4 proteins are differentially expressed in BPH and TZ cells

SULF1 and S100A4 were the most under- or over-expressed genes in BPH compared to TZ cells, respectively, and have biological functions that indicate a possible role in disease development. To determine whether SULF1 and S100A4 were differentially expressed at the protein level, we performed immunochemistry on cultured BPH and TZ stromal cells. As shown in Figure 3, SULF1 expression was significantly less in F-BPH-4 compared to F-TZ-1 cells (Figure 3E, 3F), whereas S100A4 expression was much higher in F-BPH-4 than in F-TZ-1 cells (Figure 3G, 3H). Both cell cultures showed similar uniform expression of vimentin (Figure 3A, 3B) and no staining when bovine serum albumin (BSA) was used as negative control (Figure 3C, 3D). These results demonstrated that cultured BPH and TZ stromal cells differentially expressed these two genes not only at the transcript level, but also at the protein level.

Western blotting was performed to quantify the differences in S100A4 protein expression between cultured BPH and TZ stromal cells (Figure 3I). A uniform up-regulation of S100A4 protein expression in BPH cells was observed, ranging from 7.7- to 10.7-fold, compared to that in TZ cells. Moreover, protein expression of S100A4 was also increased in the stroma of BPH tissue (Figure 4). Immunohistochemistry using paraffin-

embedded tissue sections revealed intense staining of S100A4 throughout the stroma in the tissue of origin of F-BPH-4 cells (Figure 4A, 4C), whereas only some stromal cells showed expression of S100A4 in tissue from which F-TZ-1 cells were cultured (Figure 4B, 4D). These results showed that stromal cells cultured from BPH faithfully retained the high level of expression of S100A4 that was present in the tissue of origin.

Expression of SULF1 transcripts in tissue sections were examined by in situ hybridization since antibody against SULF1 protein did not work on paraffin-embedded tissues. TZ stroma displayed strong expression of SULF1 shown by anti-sense RNA probe staining (Figure 4H), whereas little expression of SULF1 was detected in BPH stroma hybridized with the same probe (Figure 4G). No staining was observed in the stroma of BPH (Figure 4I) or TZ (Figure 4J) tissue when sense RNA probe was used. These results confirmed our findings from microarray and real time qPCR analyses and show that SULF1 is down-regulated in BPH tissue as well as in stromal cells cultured from BPH.

SULF1 enzymatic activity is down-regulated in BPH cells

To evaluate SULF1 protein activity in BPH and TZ stromal cells, we performed a functional assay to determine the enzymatic activity of SULF1 in whole cell lysates. The relative activity of SULF1 in TZ and BPH cells was calculated by normalization to the activity in the negative control, MCF-10A cells, in which no SULF1 transcript is detectable. MCF-7 cells, previously shown to possess SULF1 activity, were used as a positive control. A more than 4-fold decrease in SULF1 activity was observed in F-BPH-4 cells compared to F-TZ-1 cells (Figure 5), consistent with the decrease in SULF1 transcript in F-BPH-4 cells shown by microarray and qRT-PCR. These results

demonstrate that SULF1 is down-regulated in BPH cells at both transcript and protein function levels.

Discussion

Prostatic stromal cells cultured from tissues of different histological and pathological origins displayed distinct gene expression profiles. Many of the differentially expressed genes are involved in biological processes known to be important in the development of prostatic diseases including regulation of cell proliferation and apoptosis, cell adhesion, and immune response. SAM analysis identified genes that showed differential expression with statistical significance between two classes of samples with relevant histopathology. Our results provide a comprehensive evaluation of the gene expression profiles of cultured prostatic stromal cells, and support the hypothesis that prostatic stromal cells of different histological/pathological origins are indeed different in their transcriptional programs. This dataset also serves as a valuable resource for researchers to explore the mechanisms of actions of stromal cells in the development of BPH and prostate cancer.

Almost all prostate gene expression profiling studies have focused on molecular events associated with abnormalities in epithelial cells using either whole tissues or cultured cells (Brooks, 2002; Fromont et al., 2004; Luo et al., 2001; Nelson, 2004; Rose et al., 2005). We previously conducted one of the few gene expression profiling studies to date of prostatic stromal cells in which we investigated doxazosin-induced gene expression (Zhao et al., 2005). In that study, we only evaluated two cultures of each normal and pathological type (TZ and BPH), but nevertheless observed similar partitioning of normal TZ stromal cells from BPH stromal cells based on their gene expression patterns. In fact, when hierarchical clustering was performed using combined data for TZ and BPH cultures from our previous and current studies, a clear

separation of TZ from BPH cells was observed (unpublished data), indicating a robust difference between transcription programs in BPH vs. normal TZ stromal cells. Out of the 34 clones selected by SAM as differentially expressed between TZ and BPH cells in this study, 69% also showed differential expression in the same direction in our previous dataset. This finding also demonstrates the high reproducibility of our microarray experiments.

We compared our results with those in a recently published report by Joesting et al. of genes differentially expressed between cultures of prostate cancer-associated fibroblasts (CAFs) and normal-associated fibroblasts (NAFs) using Affymetrix microarrays (Joesting et al., 2005). In that study, 119 genes were identified with a statistically significant difference in expression between CAFs and NAFs. We found no overlap of those 119 genes with the 101 genes that we identified as differentially expressed between CA stromal cells and normal PZ stromal cells. In addition, we examined the expression of SFRP1, identified in the study by Joesting et al. as over-expressed in CAF compared to NAF and suggested to be a candidate mediator of stromal-to-epithelial signaling in prostate cancer. Our microarray analysis showed no significant difference in the expression level of SFRP1 between CA and PZ stromal cells ($p=0.06$). We also measured SFRP1 mRNA in CA and PZ stromal cells by real time qPCR and again found no significant difference in expression ($p=0.28$) (not shown).

There are several possible explanations for the differences in genes identified in these two studies. First, and maybe the most important, is that the normal stromal cells used in these two studies were perhaps different. Ours come exclusively from histologically defined PZ of the prostate, whereas the study by Joesting et al. used NAFs from undefined zonal areas (Joesting et al., 2005). When we compared gene expression

between CA stromal cells and normal stromal cells from TZ or central zone (CZ), the genes identified did not overlap with those found when normal PZ cells were used in the comparison (not shown). It appears that the anatomic origin of normal stromal cells is an important factor in such comparisons and caution needs to be taken when interpreting results from incompletely characterized cells or tissues. This is consistent with the finding of Stamey et al. who noted that different gene profiles were identified when cancer tissues were compared to normal tissues depending on which of the three zonal tissues (CZ, PZ, or TZ) were used as a control (Stamey et al., 2003). Another explanation for the different results may be the phenotypic state of the cells at the time of RNA isolation. In order to eliminate complexities related to relative states of confluency, proliferation and differentiation among the cell cultures, we followed a strict protocol of inoculating a given number of cells into nonproliferative (serum-free) medium 24 hours prior to RNA extraction. Certainly different protocols may have a significant impact on gene expression profiles. Alternatively, differences in the array platforms and statistical methods used to derive the gene lists may also contribute to the differences observed.

.

Novel genes that showed differential expression between stromal cells of BPH and TZ in our study should shed light on the role of stromal cells in the pathogenesis of BPH. The current theory is that autocrine and paracine signaling from stromal cells creates a focal area of reawakening of epithelial budding and BPH nodule formation. Although a number of factors have been implicated as mediators of such autocrine and paracrine signaling including FGF, EGF, IGF and TGF-β, the precise mechanisms that cause BPH are not clear (Lee and Peehl, 2004). Our results implicate the decreased expression of a factor, SULF1, as an important event leading to enhanced growth factor signaling in BPH. Several studies have shown that SULF1, a cell surface sulfatase, functions as a negative regulator of cell growth and that loss of SULF1 potentiates signaling of growth

factors such as hepatocyte growth factor (HGF) and FGF (Lai et al., 2003; Lai et al., 2004a; Lai et al., 2004b; Wang et al., 2004). We propose that loss of SULF1 in prostate stromal cells exerts a pro-proliferative effect in an autocrine and/or paracrine manner that leads to an overgrowth of epithelial and stromal cells. In addition, loss of SULF1 may also be related to the decreased apoptosis in BPH that has been reported (Lee and Peehl, 2004), since such an effect of decreased SULF1 expression has been reported in a number of tissues (Lai et al., 2004a; Lai et al., 2004b; Sala-Newby et al., 2005).

The theory of embryonic "reawakening" in the pathogenesis of BPH states that BPH is a process of epithelial budding and branching similar to the glandular morphogenesis that occurs in embryonic tissue as a result of stimulation from the underlying mesenchymal tissue (Isaacs and Coffey, 1989). Consistent with this theory, we observed overexpression of genes that are known components of important signaling pathways in embryonic development of the prostate. It has been shown that during ductal bud formation in rat prostate, activities of Sonic hedgehog (Shh) pathway components including the Shh receptor, Ptc1, and the members of the Gli gene family of transcriptional regulators (Gli1, Gli2, and Gli3) play a role in prostatic epithelial growth through epithelial-stromal interactions (Lamm et al., 2002; Lipinski et al., 2005). For instance, expression of Gli1, Gli2, and Gli3 was detected in the UGM during this period (Lamm et al., 2002). We observed a strong up-regulation of Gli3 at the transcript level in BPH compared to normal TZ stromal cells, suggesting a possible role of Shh signaling in promoting overgrowth of prostatic epithelium, stroma, or both in BPH nodule formation. Further investigation of the expression of target genes of the Shh pathway in BPH will help to determine the scope of involvement of Shh signaling in the pathogenesis of BPH.

Besides providing evidence to support existing theories of BPH formation, our study also provides new insights into the mechanisms that may underlie this pathological process. For instance, we observed an up-regulation of S100A4, a member of the S100 calcium-binding protein family, at both transcript and protein level in BPH compared to normal TZ stromal cells. This protein, also known as FSP1 (fibroblast-specific protein 1), is expressed by fibroblasts, possibly derived from epithelial cells through epithelial-mesenchymal transformation, during experimental tissue fibrosis (Iwano et al., 2002; Strutz et al., 1995). Its expression is also inducible by cytokines classically associated with fibrosis including EGF and TGF-β1 (Okada et al., 1997). In addition, experimental fibrogenesis can be attenuated by the selective elimination of tissue fibroblasts using a herpes virus thymidine kinase transgene under the control of the FSP1 promoter (Iwano et al., 2001). These findings provided direct evidence that FSP1-expressing fibroblasts play a crucial role in the progression of fibrosis. The up-regulation of FSP1 in BPH stromal cells that we observed indicates that molecular mechanisms underlying fibrosis may be involved in the pathogenesis of BPH. There is a large body of evidence that in BPH, the stromal-to-epithelial ratio increases up to 5:1 compared to the normal ratio of 2:1, and early nodules in the periurethral area are mostly stromal (McNeal, 1990; Shapiro et al., 1992). It is possible that this increase in the stromal volume is a result of fibrogenesis similar to that in fibrosis, and that blocking fibrosis may be effective in BPH treatment.

It is becoming accepted that the stromal microenvironment contributes to tumorigenesis in cancers of epithelial origin, including prostate cancer (Cunha et al., 2002; Cunha et al., 2003). There are a number of molecular mediators of stromal-epithelial interactions in tumorigenesis reported so far. Our study implicates ENPP2/autotaxin and lysophosphatidic acid (LPA) signaling in stromal-epithelial interaction in prostate cancer.

Autotaxin has been shown to be a potent stimulator of cancer cell motility and angiogenesis, an anti-apoptotic factor in mouse fibroblasts, and a specific target of transformation by v-JUN in chicken fibroblasts (Black et al., 2004; Hama et al., 2004; Nam et al., 2001; Song et al., 2005; Umezu-Goto et al., 2002). Because autotaxin is a key enzyme responsible for LPA generation in vivo, the observed functions of autotaxin are likely to be mediated by LPA signaling, which has been implicated in such diverse processes as wound healing, vascular remodeling, and tumor progression (Brindley, 2004; Moolenaar et al., 2004). In our study, SAM analysis showed that autotaxin is the most differentially expressed gene between CA and normal PZ stromal cells, and qRT-PCR confirmed its overexpression in CA stromal cells. This overexpression may have two consequences in the development of prostate cancer. First, autotaxin may act as an autocrine signal to promote stromal proliferation, a key element in creation of a "reactive stroma". In addition, since autotaxin is a secreted protein, it also may act as a paracrine factor in stimulating epithelial growth and angiogenesis in cancer tissues. Our findings suggest that autotaxin may be a valuable target in interventions to eliminate stromal contributions in tumor progression.

Taken together, our dataset may serve as a valuable resource for exploring molecular mechanisms underlying prostate pathogenesis. Such knowledge may also help the discovery of therapeutic targets for treatment of BPH and cancer.

Acknowledgements

Hongjuan Zhao is supported by the David W. Packard gift fund for GU Oncology. Cristiane F. Ramos is a fellow of CNPq (National Council of Scientific and Technological Development).

References

Ayala G, Tuxhorn JA, Wheeler TM, Frolov A, Scardino PT, Ohori M, Wheeler M, Spitler J, Rowley DR. 2003. Reactive stroma as a predictor of biochemical-free recurrence in prostate cancer. Clin Cancer Res 9(13):4792-4801.

Barclay WW, Woodruff RD, Hall MC, Cramer SD. 2005. A system for studying epithelial-stromal interactions reveals distinct inductive abilities of stromal cells from benign prostatic hyperplasia and prostate cancer. Endocrinology 146(1):13-18.

Black EJ, Clair T, Delrow J, Neiman P, Gillespie DA. 2004. Microarray analysis identifies Autotaxin, a tumour cell motility and angiogenic factor with lysophospholipase D activity, as a specific target of cell transformation by v-Jun. Oncogene 23(13):2357-2366.

Brindley DN. 2004. Lipid phosphate phosphatases and related proteins: signaling functions in development, cell division, and cancer. J Cell Biochem 92(5):900-912.

Brooks JD. 2002. Microarray analysis in prostate cancer research. Curr Opin Urol 12(5):395-399.

Chang HY, Sneddon JB, Alizadeh AA, Sood R, West RB, Montgomery K, Chi JT, van de Rijn M, Botstein D, Brown PO. 2004. Gene expression signature of fibroblast serum response predicts human cancer progression: similarities between tumors and wounds. PLoS Biol 2(2):E7.

Chung LW, Baseman A, Assikis V, Zhau HE. 2005. Molecular insights into prostate cancer progression: the missing link of tumor microenvironment. J Urol 173(1):10-20.

Chung LW, Cunha GR. 1983. Stromal-epithelial interactions: II. Regulation of prostatic growth by embryonic urogenital sinus mesenchyme. Prostate 4(5):503-511.

Condon MS. 2005. The role of the stromal microenvironment in prostate cancer. Semin Cancer Biol 15(2):132-137.

Cunha GR. 1984. Androgenic effects upon prostatic epitheliium are mediated via trophic influences from stroma. In: Kimball FA BA, Car DB, editor. New approaches to the study of benign prostatic hyperplasia. New Yok: Liss. p 81-102.

Cunha GR, Donjacour AA, Cooke PS, Mee S, Bigsby RM, Higgins SJ, Sugimura Y. 1987. The endocrinology and developmental biology of the prostate. Endocr Rev 8(3):338-362.

Cunha GR, Fujii H, Neubauer BL, Shannon JM, Sawyer L, Reese BA. 1983a. Epithelial-mesenchymal interactions in prostatic development. I. morphological observations of prostatic induction by urogenital sinus mesenchyme in epithelium of the adult rodent urinary bladder. J Cell Biol 96(6):1662-1670.

Cunha GR, Hayward SW, Wang YZ. 2002. Role of stroma in carcinogenesis of the prostate. Differentiation 70(9-10):473-485.

Cunha GR, Hayward SW, Wang YZ, Ricke WA. 2003. Role of the stromal microenvironment in carcinogenesis of the prostate. Int J Cancer 107(1):1-10.

Cunha GR, Reese BA, Sekkingstad M. 1980. Induction of nuclear androgen-binding sites in epithelium of the embryonic urinary bladder by mesenchyme of the urogenital sinus of embryonic mice. Endocrinology 107(6):1767-1770.

Cunha GR, Sekkingstad M, Meloy BA. 1983b. Heterospecific induction of prostatic development in tissue recombinants prepared with mouse, rat, rabbit and human tissues. Differentiation 24(2):174-180.

Fromont G, Chene L, Latil A, Bieche I, Vidaud M, Vallancien G, Mangin P, Fournier G, Validire P, Cussenot O. 2004. Molecular profiling of benign prostatic hyperplasia using a large scale real-time reverse transcriptase-polymerase chain reaction approach. J Urol 172(4 Pt 1):1382-1385.

Hama K, Aoki J, Fukaya M, Kishi Y, Sakai T, Suzuki R, Ohta H, Yamori T, Watanabe M, Chun J, Arai H. 2004. Lysophosphatidic acid and autotaxin stimulate cell motility of neoplastic and non-neoplastic cells through LPA1. J Biol Chem 279(17):17634-17639.

Hayward SW, Wang Y, Cao M, Hom YK, Zhang B, Grossfeld GD, Sudilovsky D, Cunha GR. 2001. Malignant transformation in a nontumorigenic human prostatic epithelial cell line. Cancer Res 61(22):8135-8142.

Isaacs JT, Coffey DS. 1989. Etiology and disease process of benign prostatic hyperplasia. Prostate Suppl 2:33-50.

Iwano M, Fischer A, Okada H, Plieth D, Xue C, Danoff TM, Neilson EG. 2001. Conditional abatement of tissue fibrosis using nucleoside analogs to selectively corrupt DNA replication in transgenic fibroblasts. Mol Ther 3(2):149-159.

Iwano M, Plieth D, Danoff TM, Xue C, Okada H, Neilson EG. 2002. Evidence that fibroblasts derive from epithelium during tissue fibrosis. J Clin Invest 110(3):341-350.

Joesting MS, Perrin S, Elenbaas B, Fawell SE, Rubin JS, Franco OE, Hayward SW, Cunha GR, Marker PC. 2005. Identification of SFRP1 as a candidate mediator of stromal-to-epithelial signaling in prostate cancer. Cancer Res 65(22):10423-10430.

Lai J, Chien J, Staub J, Avula R, Greene EL, Matthews TA, Smith DI, Kaufmann SH, Roberts LR, Shridhar V. 2003. Loss of HSulf-1 up-regulates heparin-binding growth factor signaling in cancer. J Biol Chem 278(25):23107-23117.

Lai JP, Chien J, Strome SE, Staub J, Montoya DP, Greene EL, Smith DI, Roberts LR, Shridhar V. 2004a. HSulf-1 modulates HGF-mediated tumor cell invasion and signaling in head and neck squamous carcinoma. Oncogene 23(7):1439-1447.

Lai JP, Chien JR, Moser DR, Staub JK, Aderca I, Montoya DP, Matthews TA, Nagorney DM, Cunningham JM, Smith DI, Greene EL, Shridhar V, Roberts LR. 2004b. hSulf1 Sulfatase promotes apoptosis of hepatocellular cancer cells by decreasing heparin-binding growth factor signaling. Gastroenterology 126(1):231-248.

Lamm ML, Catbagan WS, Laciak RJ, Barnett DH, Hebner CM, Gaffield W, Walterhouse D, Iannaccone P, Bushman W. 2002. Sonic hedgehog activates mesenchymal Gli1 expression during prostate ductal bud formation. Dev Biol 249(2):349-366.

Lee KL, Peehl DM. 2004. Molecular and cellular pathogenesis of benign prostatic hyperplasia. J Urol 172(5 Pt 1):1784-1791.

Lipinski RJ, Cook CH, Barnett DH, Gipp JJ, Peterson RE, Bushman W. 2005. Sonic hedgehog signaling regulates the expression of insulin-like growth factor binding protein-6 during fetal prostate development. Dev Dyn 233(3):829-836.

Luo J, Duggan DJ, Chen Y, Sauvageot J, Ewing CM, Bittner ML, Trent JM, Isaacs WB. 2001. Human prostate cancer and benign prostatic hyperplasia: molecular dissection by gene expression profiling. Cancer Res 61(12):4683-4688.

McNeal J. 1990. Pathology of benign prostatic hyperplasia. Insight into etiology. Urol Clin North Am 17(3):477-486.

McNeal JE. 1978. Origin and evolution of benign prostatic enlargement. Invest Urol 15(4):340-345.

Moolenaar WH, van Meeteren LA, Giepmans BN. 2004. The ins and outs of lysophosphatidic acid signaling. Bioessays 26(8):870-881.

Nam SW, Clair T, Kim YS, McMarlin A, Schiffmann E, Liotta LA, Stracke ML. 2001. Autotaxin (NPP-2), a metastasis-enhancing motogen, is an angiogenic factor. Cancer Res 61(18):6938-6944.

Nelson PS. 2004. Predicting prostate cancer behavior using transcript profiles. J Urol 172(5 Pt 2):S28-32; discussion S33.

Okada H, Danoff TM, Kalluri R, Neilson EG. 1997. Early role of Fsp1 in epithelial-mesenchymal transformation. Am J Physiol 273(4 Pt 2):F563-574.

Peehl DM, Sellers RG. 2000. Cultured stromal cells: an in vitro model of prostatic mesenchymal biology. Prostate 45(2):115-123.

Rose A, Xu Y, Chen Z, Fan Z, Stamey TA, McNeal JE, Caldwell M, Peehl DM. 2005. Comparative gene and protein expression in primary cultures of epithelial cells from benign prostatic hyperplasia and prostate cancer. Cancer Lett 227(2):213-222.

Sala-Newby GB, George SJ, Bond M, Dhoot GK, Newby AC. 2005. Regulation of vascular smooth muscle cell proliferation, migration and death by heparan sulfate 6-O-endosulfatase1. FEBS Lett 579(28):6493-6498.

San Francisco IF, DeWolf WC, Peehl DM, Olumi AF. 2004. Expression of transforming growth factor-beta 1 and growth in soft agar differentiate prostate carcinoma-associated fibroblasts from normal prostate fibroblasts. Int J Cancer 112(2):213-218.

Shapiro E, Becich MJ, Hartanto V, Lepor H. 1992. The relative proportion of stromal and epithelial hyperplasia is related to the development of symptomatic benign prostate hyperplasia. J Urol 147(5):1293-1297.

Sherlock G, Hernandez-Boussard T, Kasarskis A, Binkley G, Matese JC, Dwight SS, Kaloper M, Weng S, Jin H, Ball CA, Eisen MB, Spellman PT, Brown PO, Botstein D, Cherry JM. 2001. The Stanford Microarray Database. Nucleic Acids Res 29(1):152-155.

Song J, Clair T, Noh JH, Eun JW, Ryu SY, Lee SN, Ahn YM, Kim SY, Lee SH, Park WS, Yoo NJ, Lee JY, Nam SW. 2005. Autotaxin (lysoPLD/NPP2) protects fibroblasts from apoptosis through its enzymatic product, lysophosphatidic acid, utilizing albumin-bound substrate. Biochem Biophys Res Commun 337(3):967-975.

Stamey TA, Caldwell MC, Fan Z, Zhang Z, McNeal JE, Nolley R, Chen Z, Mahadevappa M, Warrington JA. 2003. Genetic profiling of Gleason grade 4/5 prostate cancer: which is the best prostatic control tissue? J Urol 170(6 Pt 1):2263-2268.

Strutz F, Okada H, Lo CW, Danoff T, Carone RL, Tomaszewski JE, Neilson EG. 1995. Identification and characterization of a fibroblast marker: FSP1. J Cell Biol 130(2):393-405.

Tusher VG, Tibshirani R, Chu G. 2001. Significance analysis of microarrays applied to the ionizing radiation response. Proc Natl Acad Sci U S A 98(9):5116-5121.

Tuxhorn JA, Ayala GE, Rowley DR. 2001. Reactive stroma in prostate cancer progression. J Urol 166(6):2472-2483.

Tuxhorn JA, Ayala GE, Smith MJ, Smith VC, Dang TD, Rowley DR. 2002a. Reactive stroma in human prostate cancer: induction of myofibroblast phenotype and extracellular matrix remodeling. Clin Cancer Res 8(9):2912-2923.

Tuxhorn JA, McAlhany SJ, Dang TD, Ayala GE, Rowley DR. 2002b. Stromal cells promote angiogenesis and growth of human prostate tumors in a differential reactive stroma (DRS) xenograft model. Cancer Res 62(11):3298-3307.

Umezu-Goto M, Kishi Y, Taira A, Hama K, Dohmae N, Takio K, Yamori T, Mills GB, Inoue K, Aoki J, Arai H. 2002. Autotaxin has lysophospholipase D activity leading to tumor cell growth and motility by lysophosphatidic acid production. J Cell Biol 158(2):227-233.

Wang S, Ai X, Freeman SD, Pownall ME, Lu Q, Kessler DS, Emerson CP, Jr. 2004. QSulf1, a heparan sulfate 6-O-endosulfatase, inhibits fibroblast growth factor signaling in mesoderm induction and angiogenesis. Proc Natl Acad Sci U S A 101(14):4833-4838.

West RB, Corless CL, Chen X, Rubin BP, Subramanian S, Montgomery K, Zhu S, Ball CA, Nielsen TO, Patel R, Goldblum JR, Brown PO, Heinrich MC, van de Rijn M. 2004. The novel marker, DOG1, is expressed ubiquitously in gastrointestinal stromal tumors irrespective of KIT or PDGFRA mutation status. Am J Pathol 165(1):107-113.

Zhao H, Lai F, Nonn L, Brooks JD, Peehl DM. 2005. Molecular targets of doxazosin in human prostatic stromal cells. Prostate 62(4):400-410.

Figure legends

Figure 1. Hierarchical clustering analysis of genes differentially expressed in prostatic stromal cells. (A) Overview of relative expression levels of 714 genes represented by 1,032 clones whose expression varied at least threefold from the mean abundance in at least three samples in all 18 stromal cell cultures. Each column represents data from a single stromal cell culture, and each row represents expression levels for a single gene across the 18 samples. Transcripts up-regulated were in red and down-regulated in green. The degree of color saturation corresponds with the ratio of gene expression shown at the bottom of the image. Full transcript identities and raw data are available at http://www.Stanford.edu/~hongjuan/stromal. In the dendrogram shown on top of the image, BPH cells were colored in blue, cancer cells in red, PZ cells in green, and TZ cells in purple. The same color code was used in (B)-(D). (B) Dendrogram of clustering analysis using the 1032 clones described in (A). (C) Dendrogram of clustering analysis using 455 clones representing 361 genes whose expression varied at least threefold from the mean abundance in at least four samples in all 18 stromal cell cultures. (D) Dendrogram of clustering analysis using 232 clones representing 192 genes whose expression varied at least fourfold from the mean abundance in at least four samples in all 18 stromal cell cultures.

Figure 2. Validation of gene expression changes observed using microarray by real time RT-PCR. Levels of transcripts of interest determined by PT-PCR in triplicates were normalized against that of TBP in the same sample. For comparison, expression levels in F-BPH-1 were scaled to 1, except for BST1, for which expression level in F-CA-4 was scaled to 1.

Figure 3. Comparison of SULF1 and S100A4 expression in cultured BPH and TZ cells by immunochemistry (A-H) and western blotting (I). SULF1 expression is significantly less in F-BPH-4 cells (E) compared to F-TZ-1 cells (F), whereas S100A4 expression is much higher in F-BPH-4 cells (G) than in F-TZ-1 cells (H). Both cell cultures showed similar uniform expression of vimentin (A, B) and no staining when BSA was used as negative control (C, D). Western blotting (I) showed S100A4 expression was decreased in BPH cells, ranging from 7.7- to 10.7-fold, compared to TZ cells.

Figure 4. Comparison of S100A4 and SULF1 expression in tissue sections of BPH and TZ. Intense staining of S100A4 by immunohistochemistry was observed throughout the stromal area of BPH tissue from which the cell culture, F-BPH-4, was derived (A), whereas only some stromal cells showed expression of S100A4 in the normal TZ tissue from which F-TZ-1 was derived (B). (C) and (D) are higher magnification of (A) and (B), respectively. (E) and (F) are negative controls stained with BSA. In situ hybridization using anti-sense RNA probe against SULF1 showed that SULF1 transcript is present at high levels in the stroma of normal TZ tissue (H), but not in BPH stroma (G), whereas sense RNA probe didn't show labeling in either BPH (I) or TZ (J) stroma.

Figure 5. Sulfatase assay in cultured BPH and TZ stromal cells. Relative activity was calculated by scaling the activity in MCF-10A cells, the negative control, to 1. MCF-7 cells were used as a positive control. F-BPH-4 cells showed a more than 4-fold decrease in SULF1 activity compared to F-TZ-1 cells.

Table 1 Summary of cell cultures used in the study

Name	Age of Donor	Passage number	Histology
F-BPH-1	63	10	BPH
F-BPH-2	55	11	BPH
F-BPH-3	65	14	BPH
F-BPH-4	58	8	BPH
F-TZ-1	43	16	Normal TZ
F-TZ-2	62	14	Normal TZ
F-CA-1	57	11	CA 4/3
F-CA-2	69	10	CA 3/4
F-CA-3	58	10	CA 3/4
F-CA-4	59	14	CA 3/3
F-CA-5	65	14	CA 4/3
F-PZ-1	67	15	Normal PZ
F-PZ-2	58	16	Normal PZ
F-PZ-3	66	11	Normal PZ
F-PZ-4	66	4	Normal PZ
F-PZ-5	59	11	Normal PZ
F-PZ-6	66	15	Normal PZ
F-PZ-7	59	17	Normal PZ

Table 2 Genes differentially expressed in BPH compared to TZ stromal cells identified by SAM

Symbol	Fold change	SAM rank	GO annotation
Down-regulated in BPH			
SULF1	-3.8	1	apoptosis
TGFB2	-4.2	2	cell proliferation/cell cycle
LASS6	-5.0	3	regulation of transcription
Up-regulated in BPH			
S100A4	10.8	1	calcium ion binding
TOX	34.2	2	regulation of transcription
BUB1	19.7	3	cell cycle/cell proliferation
CLDN23	6.0	7	cell-cell adhesion
OAS2	6.7	8	immune response
IF	5.4	9	immune response
GBP2	15.3	11	immune response
DNAJC4	3.0	12	protein folding
GLI3	45.8	13	regulation of transcription/signal transduction
SOX12	3.6	14	RNA polymerase II transcription factor activity
AIM1	6.6	15	sugar binding
DKFZP586A0522	5.0	16	methyltransferase activity
S100A10	4.9	17	calcium ion binding
PLGL	5.8	19	plasmin activity
PLEKHC1	3.2	20	cell adhesion
RPS6KL1	3.2	22	structural constituent of ribosome
TEAD3	2.8	25	regulation of transcription
BST1	2.8	28	humoral immune response

Table 3 Genes differentially expressed in BPH compared to CA stromal cells identified by SAM

Symbol	Fold change	SAM rank	GO annotation
		Up-regulated in CA	
BACE2	5.0	1	peptide hormone processing
SULF1	4.4	2	apoptosis
OGN	7.1	3	growth factor activity
MGP	2.3	4	cell differentiation
DOCK10	4.4	5	guanyl-nucleotide exchange factor activity
THY1	3.4	6	cell surface antigen
		Up-regulated in BPH	
BST1	4.2	1	humoral immune response
ARHGAP28	3.8	2	viral release
OLR1	2.3	3	proteolysis and peptidolysis
COL4A5	5.0	4	extracellular matrix structural constituent
TOX	5.0	6	regulation of transcription
IGF2	10.2	7	cell proliferation/regulation of cell cycle
SLC6A6	6.1	8	taurine:sodium symporter activity
TEK	6.4	9	cell-cell signaling/signal transduction
KMO	2.5	10	electron transport
C11orf30	2.0	11	DNA repair/regulation of transcription
LOC492304	6.7	12	insulin-like growth factor binding
TBL1X	2.5	14	regulation of transcription
CHN1	3.7	15	GTPase activator activity
SLC4A4	5.7	16	sodium:bicarbonate symporter activity
MFHAS1	2.3	17	small GTPase mediated signal transduction
TERF1	2.0	18	cell cycle/regulation of transcription
FARP1	2.1	19	Rho guanyl-nucleotide exchange factor activity
MPP3	3.5	20	guanylate kinase activity/signal transduction
VAMP5	2.8	21	cell differentiation/vesicle-mediated transport
SSH2	2.2	22	protein amino acid dephosphorylation
GTF2E1	1.9	24	regulation of transcription
SIPA1L2	2.6	27	GTPase activator activity
NRG2	6.4	28	anti-apoptosis/cell-cell signaling
MYO6	2.0	29	ATPase activity/structural constituent of muscle

Table 4 Genes up-regulated in CA compared to PZ stromal cells identified by SAM

Symbol	Fold change	SAM rank	GO annotation
ENPP2	7.4	1	chemotaxis/transcription factor binding
TM4SF3	3.6	2	signal transducer activity
SEPT6	3.7	6	cell cycle
ICAM4	2.3	8	cell-cell adhesion
LOC91431	1.8	12	zinc ion binding
ADCK1	2.4	13	protein amino acid phosphorylation
DLL3	3.3	15	cell fate determination
CMRF35	2.9	16	cellular defense response
P2RY1	1.8	18	G-protein signaling
LRRC7	2.0	19	protein binding
DYRK2	1.9	21	protein amino acid phosphorylation
LOC400713	1.9	22	regulation of transcription
WDR7	2.2	23	cell cycle/apoptosis
NAGA	2.9	25	carbohydrate metabolism
NF1	2.3	27	Ras protein signal transduction/cell cycle
C16orf34	2.4	28	regulation of transcription
HSPD1	2.0	29	response to unfolded protein
MICAL2	2.3	30	electron transport
C6orf68	2.4	31	metabolism|transferase activity
IGF1	1.9	32	positive regulation of cell proliferation
BCL2A1	2.5	34	anti-apoptosis
CRY1	2.1	36	DNA repair/G-protein coupled photoreceptor activity
FRAG1	1.6	37	receptor activity
NISCH	1.7	38	intracellular signaling cascade
FBXW8	2.1	39	ubiquitin cycle
TRIM33	1.7	40	regulation of transcription/ubiquitin-protein ligase activity
PDE3B	2.0	41	signal transduction
LMO2	4.4	42	zinc ion binding
SLC5A8	1.8	45	transporter activity
UGT2B7	4.2	49	lipid metabolism
MCM5	2.6	51	regulation of cell cycle/regulation of transcription
TAC1	2.7	52	cell-cell signaling
SPRY3	2.0	54	regulation of signal transduction
LTB4R	1.8	55	inflammatory response/signal transduction
PKIB	3.7	56	cAMP-dependent protein kinase inhibitor activity
KCTD13	1.8	59	voltage-gated potassium channel activity
ATF6	1.8	64	regulation of transcription/signal transduction
EBF	1.9	65	regulation of transcription
MARCH-I	2.2	66	protein ubiquitination
PANX2	1.7	67	gap junction
FLJ22405	2.2	68	protein amino acid dephosphorylation
LGR4	1.9	69	G-protein coupled receptor protein signaling pathway
XAB1	2.3	71	small GTPase mediated signal transduction
CA12	2.7	72	one-carbon compound metabolism

Symbol	Fold change	SAM rank	GO annotation
MUC5B	1.9	74	cell adhesion
RERG	1.9	75	cell proliferation/signal transduction
LOC126295	1.7	76	regulation of transcription
GATA6	3.7	77	regulation of transcription
FGFR1	1.9	78	cell growth/FGF receptor signaling pathway
ARGBP2	2.1	79	structural constituent of muscle
ERBB2	1.8	81	cell proliferation
COL4A2	1.9	83	cell adhesion
NUP160	2.0	84	mRNA-nucleus export
LIMS3	3.2	85	zinc ion binding
AKR1B10	2.1	86	aldehyde metabolism/electron transporter
OGN	1.9	88	growth factor activity
NRK	1.9	89	small GTPase regulator activity
RPL27A	1.8	91	structural constituent of ribosome
TRPM3	1.7	92	calcium ion transport
DCAMKL1	5.8	93	cell differentiation
KCNIP4	1.7	94	calcium ion binding
KCNC4	3.8	95	cation transport
IGSF10	1.9	97	vascular endothelial growth factor receptor activity
GSTZ1	1.8	98	tyrosine catabolism
ZNF367	2.1	99	nucleic acid binding
PON1	5.8	100	aryldialkylphosphatase activity
HSPB6	3.0	101	response to unfolded protein

Table 5 Validation of gene expression by qRT-PCR

Symbol	Fold change	SAM rank	P value (≤ 0. 05)
BPH vs. TZ			
SULF1	↓5.1	1	Yes
TGFB2	↓1.4	2	*No*
LASS6	↓5.1	3	Yes
S100A4	↑9.3	1	Yes
TOX	↑5.5	2	Yes
BUB1	↑3.4	3	*No*
CLDN23	↑4.6	7	Yes
OAS2	↑2.0	8	*No*
IF	↑5.3	9	Yes
GBP2	↑11.6	11	Yes
DNAJC4	↑1.1	12	*No*
GLI3	↑9.4	13	Yes
S100A10	↑5.5	17	Yes
BST1	↑1.4	28	*No*
BPH vs. CA			
SULF1	↓4.6	2	*No*
OGN	↓10.0	3	Yes
THY1	↓3.8	6	Yes
BST1	↑3.3	1	Yes
TOX	↑3.4	6	Yes
IGF2	↑9.9	7	Yes
LOC492304	↑9.6	12	Yes
CA vs. PZ			
ENPP2	↑2.7	1	Yes
WDR7	↓1.1	23	*No*
IGF1	↓1.4	32	*No*
BCL2A1	↑7.7	34	*No*
FRAG1	1.0	37	*No*
FGFR1	↓1.3	78	*No*
OGN	↑5.8	88	Yes
PON1	↑1.3	100	*No*

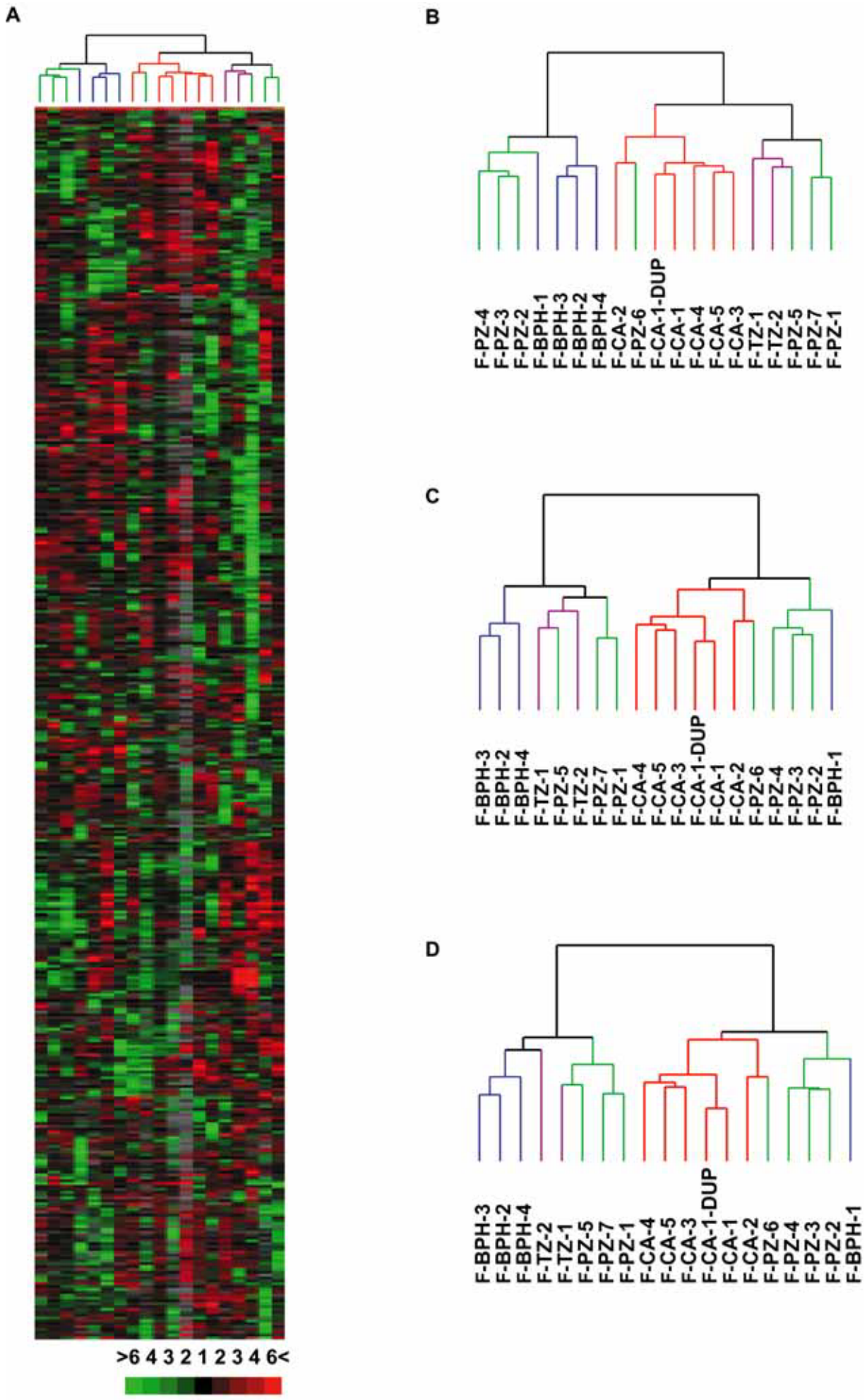
A
>6 4 3 2 1 2 3 4 6<
B
F-PZ-4
F-PZ-3
F-PZ-2
F-BPH-1
F-BPH-3
F-BPH-2
F-BPH-4
F-CA-2
F-PZ-6
F-CA-1-DUP
F-CA-1
F-CA-4
F-CA-5
F-CA-3
F-TZ-1
F-TZ-2
F-PZ-5
F-PZ-7
F-PZ-1
C
F-BPH-3
F-BPH-2
F-BPH-4
F-TZ-1
F-PZ-5
F-TZ-2
F-PZ-7
F-PZ-1
F-CA-4
F-CA-5
F-CA-3
F-CA-1-DUP
F-CA-1
F-CA-2
F-PZ-6
F-PZ-4
F-PZ-3
F-PZ-2
F-BPH-1
D
F-BPH-3
F-BPH-2
F-BPH-4
F-TZ-2
F-TZ-1
F-PZ-5
F-PZ-7
F-PZ-1
F-CA-4
F-CA-5
F-CA-3
F-CA-1-DUP
F-CA-1
F-CA-2
F-PZ-6
F-PZ-4
F-PZ-3
F-PZ-2
F-BPH-1

Figure 1

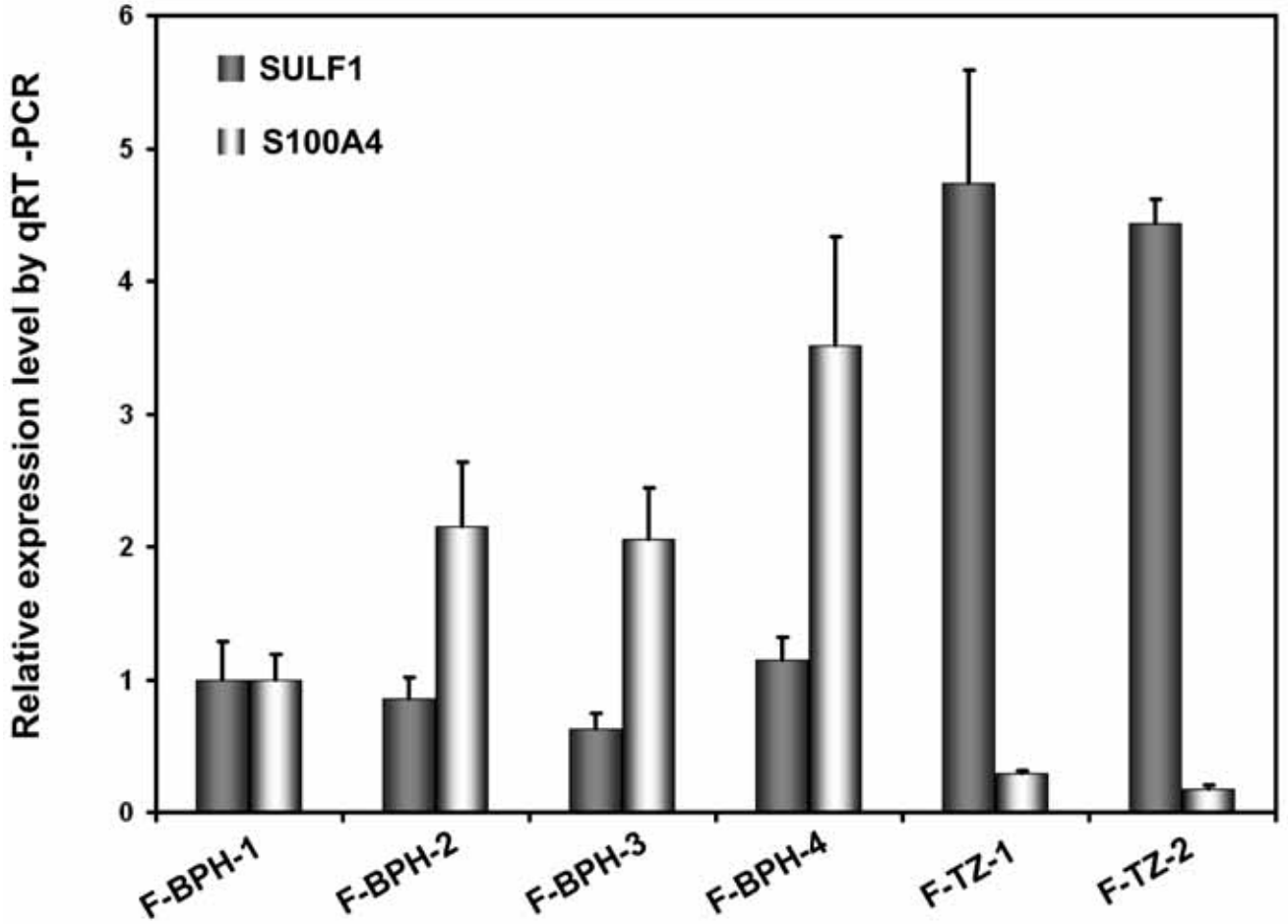
SULF1
S100A4
Relative expression level by qRT -PCR
0
1
2
3
4
5
6
F-BPH-1
F-BPH-2
F-BPH-3
F-BPH-4
F-TZ-1
F-TZ-2

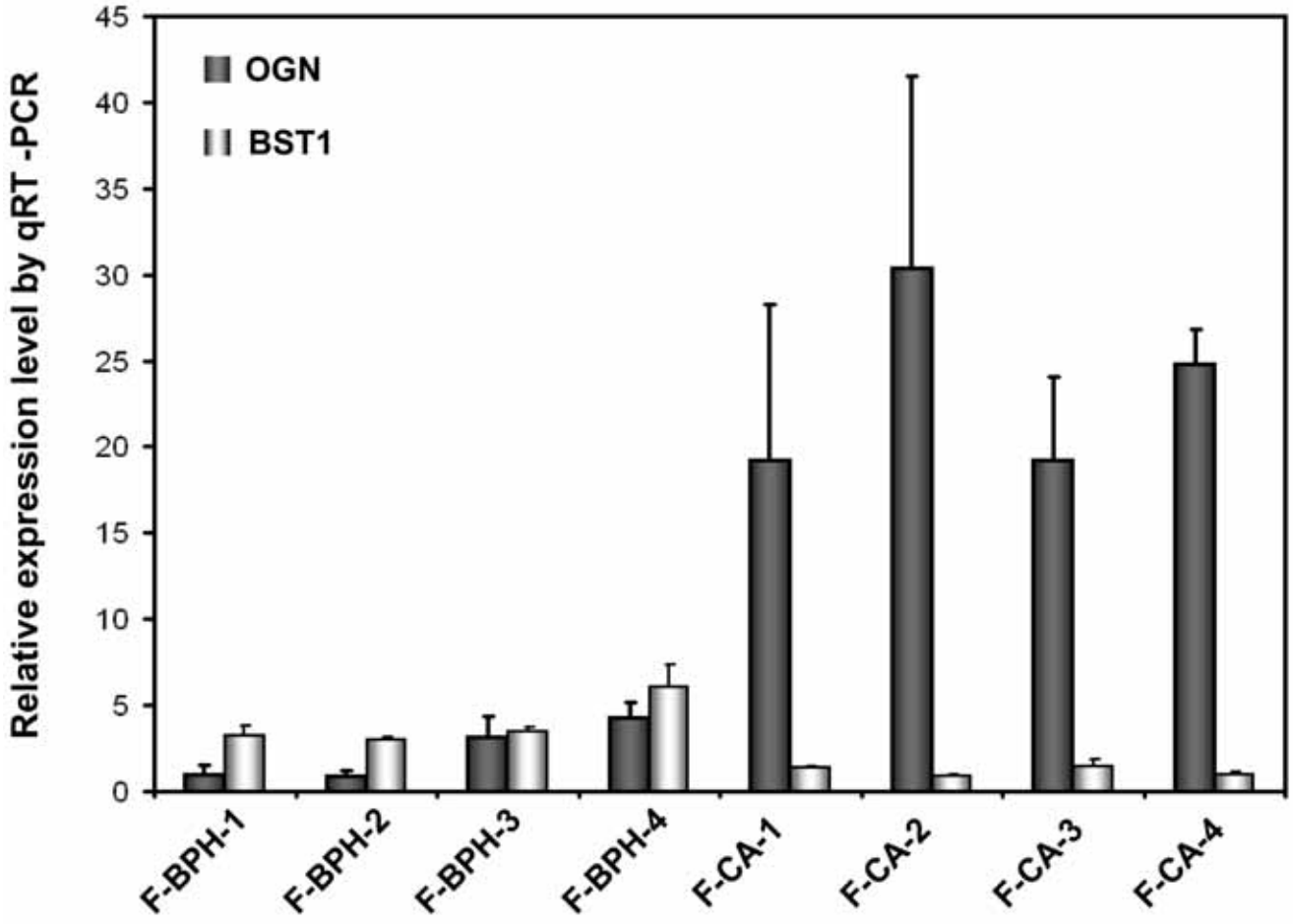
OGN
BST1
Relative expression level by qRT -PCR
0
5
10
15
20
25
30
35
40
45
F-BPH-1
F-BPH-2
F-BPH-3
F-BPH-4
F-CA-1
F-CA-2
F-CA-3
F-CA-4

Figure 2

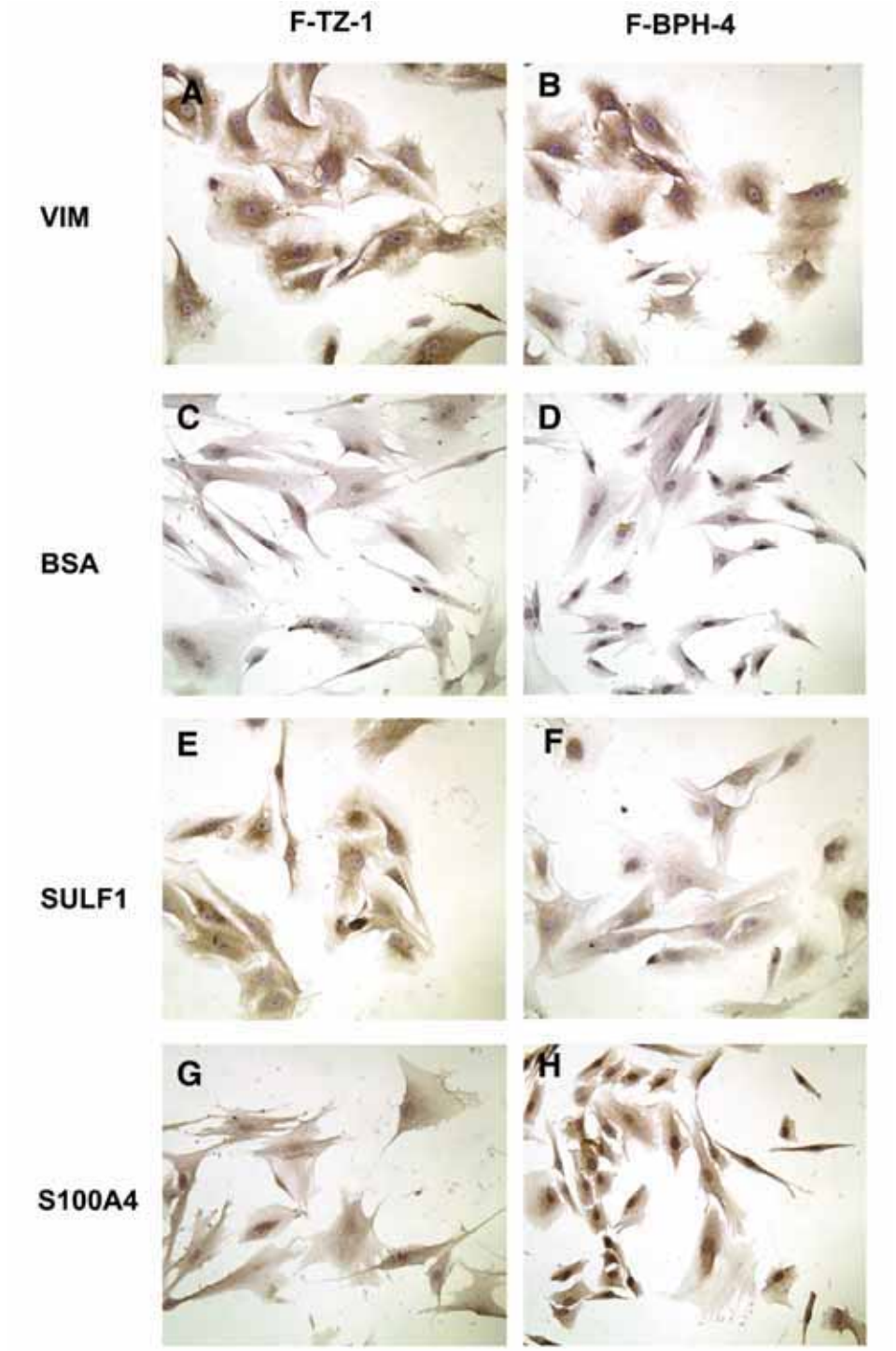
F-TZ-1
F-BPH-4
VIM
BSA
SULF1
S100A4
A
B
C
D
E
F
G
H

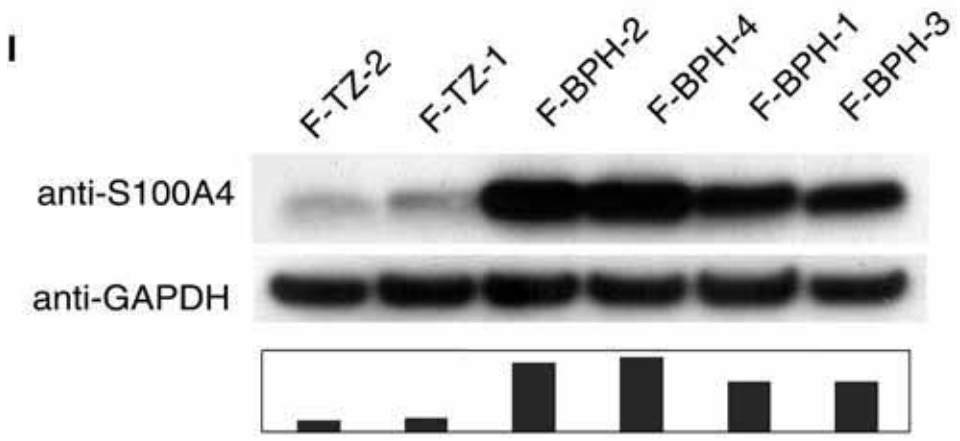
I
F-TZ-2
F-TZ-1
F-BPH-2
F-BPH-4
F-BPH-1
F-BPH-3
anti-S100A4
anti-GAPDH

Figure 3

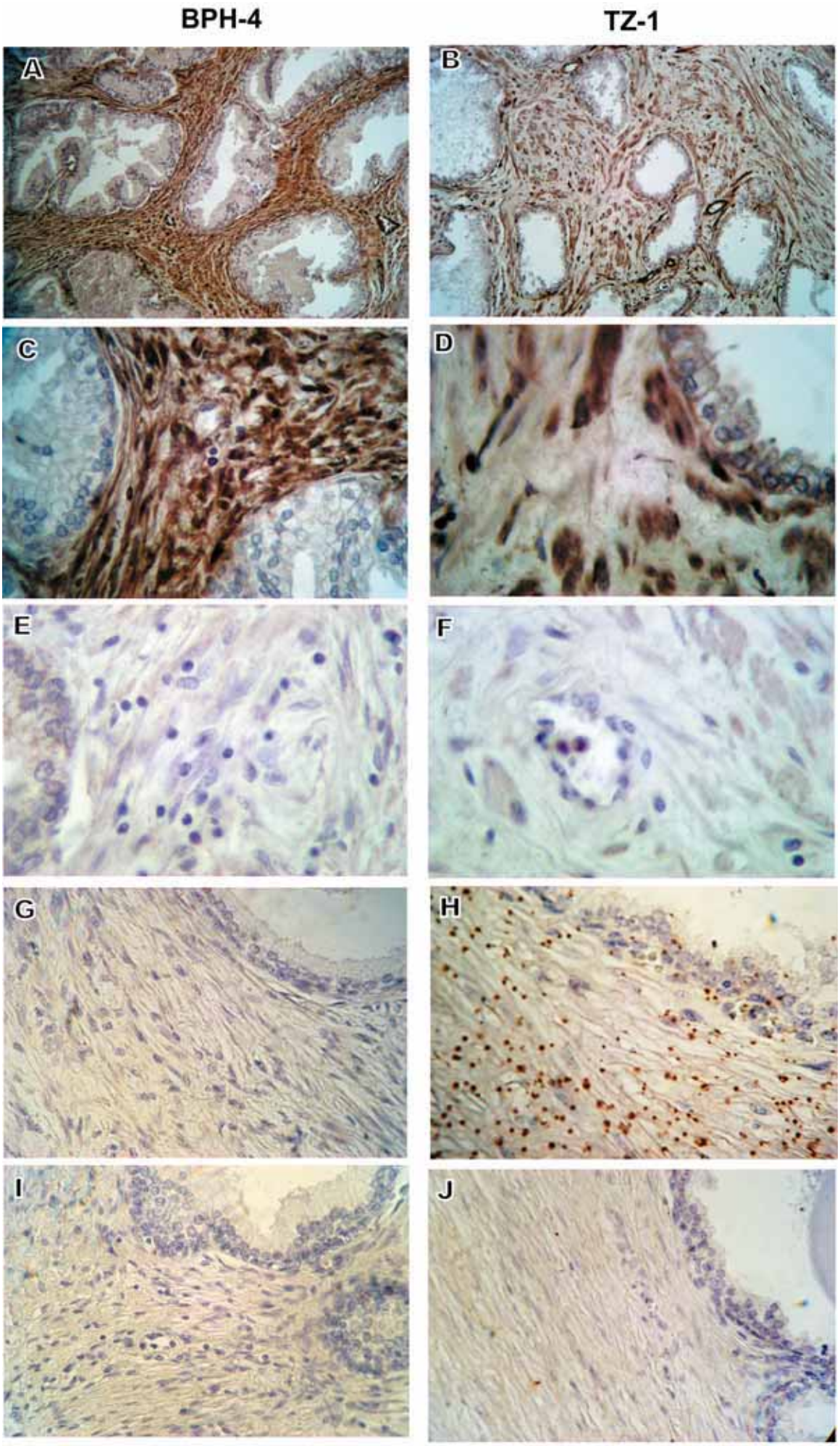

Figure 4

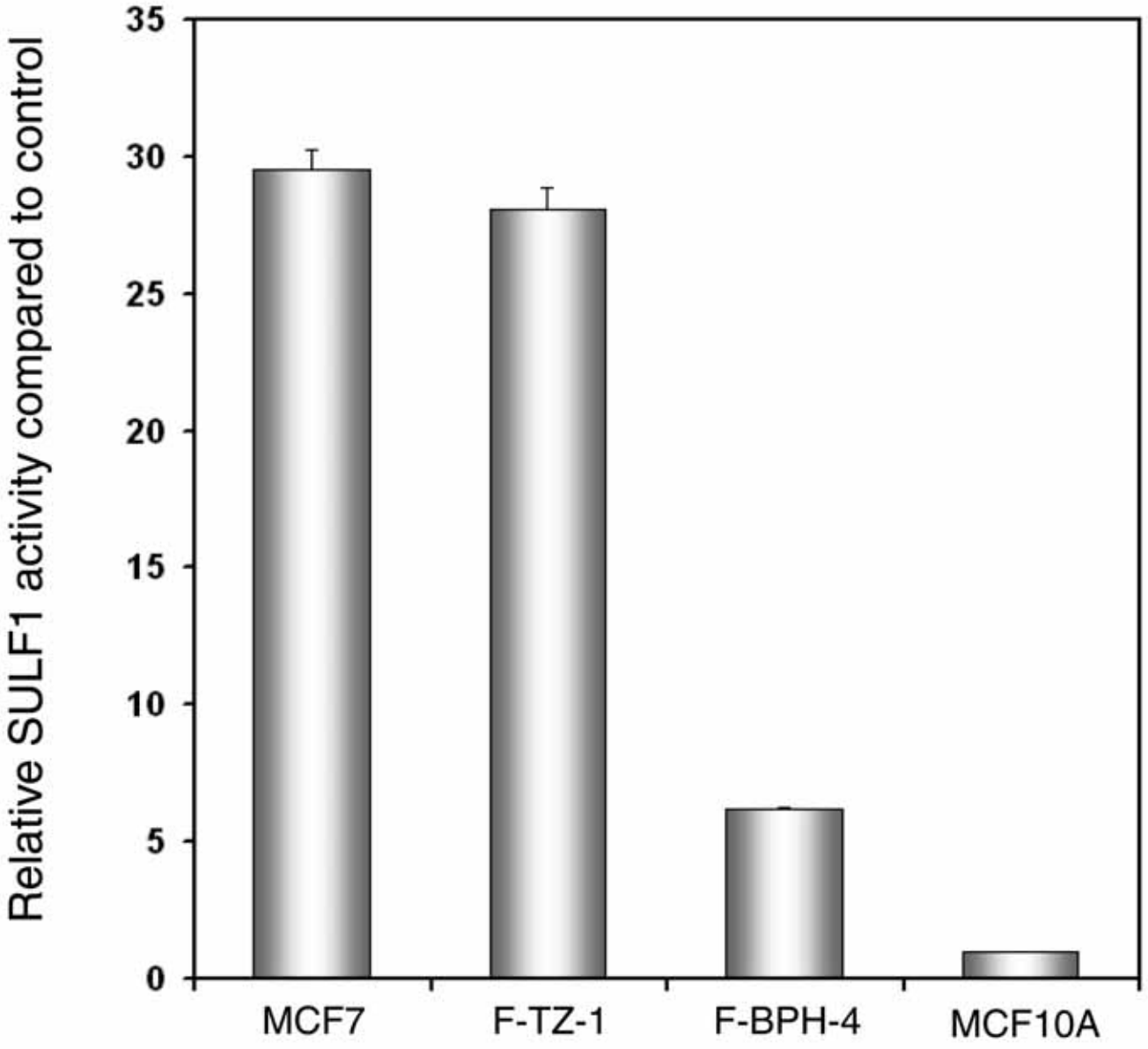
Relative SULF1 activity compared to control
35
30
25
20
15
10
5
0
MCF7
F-TZ-1
F-BPH-4
MCF10A

Figure 5

name	target gene	sequence
BCL2A1-1	BCL2A1	agcaaaacgtccagagtgct
BCL2A1-2	BCL2A1	cccagttaatgatgccgtct
BST1-1	BST1	cgattaccaatcctgcccta
BST1-2	BST1	tttgatgggataggctcctg
BUB1-1	BUB1	cctttggagaacgctctgtc
BUB1-2	BUB1	tgtgaagtctcctgggctct
CLDN23-1	CLDN23	tccgacctctagacgcttgt
CLDN23-2	CLDN23	gaaaggcagatttccatcca
DNAJC4-1	DNAJC4	acgaaccacagtccatgaca
DNAJC4-2	DNAJC4	ccccagcacttgtttgtttt
ENPP2-1	ENPP2	acaacgaggagagctgcaat
ENPP2-2	ENPP2	agaagtccaggctggtgaga
FGFR1-1	FGFR1	cgatgtgcagafcatcaact
FGFR1-2	FGFR1	tgctggttacgcaagcatag
FRAG1-1	FRAG1	cctgctcttccacttcaagg
FRAG1-2	FRAG1	gcagctgaggtagtggttcc
GBP2-1	GBP2	gatttcaccctggaactgga
GBP2-2	GBP2	gacgaagcacttcctcttgg
GLI3-1	GLI3	ctttgcaagccaggagaaac
GLI3-2	GLI3	tgttggactgtgtgccattt
IF-1	IF	gaaacgaattgtgggaggaa
IF-2	IF	gcagcagtcagaatccaaca
IGF1-1	IGF1	cagcagtcttccaacccaat
IGF1-2	IGF1	cacgaactgaagagcatcca
IGF2-1	IGF2	atgacacctggaagcagtcc
IGF2-2	IGF2	cttgggtgggtagagcaatc
LASS6-1	LASS6	ttcgacaaagacgcaatcag
LASS6-2	LASS6	agcaatgcctcgtattccac
LOC492304-1	LOC492304	attggacagaagcccaaaga
LOC492304-2	LOC492304	ctgacgaatgggcaggtaat
OAS2-1	OAS2	tcagcgaggccagtaatctt
OAS2-2	OAS2	gcaggacattccaagatggt
OGN-1	OGN	tggaatccgtgcctcttaat
OGN-2	OGN	tggtgtcattagccttgcag
PON1-1	PON1	agaggtgcttcgaatccaga
PON1-2	PON1	aacactgtgccaatcagcag
S100A10-1	S100A10	gggcttccagagcttctttt
S100A10-2	S100A10	cttctatgggggaagctgtg
S100A4-1	S100A4	gatgagcaacttggacagca
S100A4-2	S100A4	cttcctgggctgcttatctg
SOX12-1	SOX12	gcccatcgtgttactccatt
SOX12-2	SOX12	gcttcaccaggaagcagaac
SULF1-1	SULF1	aagtgacgggttcttggttg
SULF1-2	SULF1	ggcaaggtcaaatgaggtgt
TGFB2-1	TGFB2	cgccaaggaggtttacaaaa
TGFB2-2	TGFB2	ctccattgctgagacgtcaa
THY1-1	THY1	ctagtggaccagagccttcg
THY1-2	THY1	gcacgtgcttctttgtctca
TOX-1	TOX	tatcaccaacaaccgggaat
TOX-2	TOX	gtgctgctgcatgttgagat
WDR7-1	WDR7	tcaatggatgtgtccgctgt
WDR7-2	WDR7	ttggctatggtggtgatgaa

Transcript profiling of the androgen signal in normal prostate, benign prostatic hyperplasia and prostate cancer*

David R. Bauman[1], Stephan Steckelbroeck[1], Donna M. Peehl[2] and Trevor M. Penning[1]

From the [1]Department of Pharmacology, University of Pennsylvania School of Medicine, Philadelphia, PA 19104-6084 and [2]Department of Urology, Stanford University School of Medicine, Stanford, CA 94305

Running title: Transcript profiles in prostate diseases.

Address correspondence to: Trevor M. Penning, Department of Pharmacology, University of Pennsylvania School of Medicine, 130C John Morgan Building, 3620 Hamilton Walk, Philadelphia, PA 19104-6084, USA. Tel.: 215-898-9445; Fax: 215-573-2236; E-mail: penning@pharm.med.upenn.edu

Number of tables # 1

Number of figures # 9 (6 total)

Number of references # (50 max)

Number of words in the abstract # 247 (250 max)

Number of words # 5024 (5000 max)

Key words: aldo-keto reductases, hydroxysteroid dehydrogenases, type 2 5α-reductase, androgen receptor, estrogen receptor.

*This work was supported by R01 CA-90744 awarded to T.M.P., DAMD PC040420 awarded to D.M.P. and D.R.B. was supported in part by training Grant 1R25-CA 101871-D1.

The abbreviations used are: prostate adenocarcinoma (CaP), benign prostatic hyperplasia (BPH), 5α-dihydrotestosterone (DHT), 5α-androstane-3α,17β-diol (3α-diol), 5α-androstane-3β,17β-diol (3β-diol), Δ^4-androstene-3,17-dione (androstenedione), 17β-hydroxy-androst-4-ene-3-one (testosterone), hydroxysteroid dehydrogenase (HSD), androgen receptor (AR), retinol dehydrogenase- like 3α-HSD (RL-HSD), 11-*cis* retinol dehydrogenase (RODH 5), L-3-hydroxyacyl coenzyme A dehydrogenase/Type 10 17β-HSD (ERAB), novel type of human microsomal 3α-HSD (NT 3α-HSD), retinol dehydrogenase 4 (RODH 4), cytochrome P450 7B1 (P4507B1), estrogen receptor α (ERα), estrogen receptor β (ERβ), 20α-HSD (AKR1C1), type 3 3α-HSD (AKR1C2), type 2 3α-HSD/type 5 17β-HSD (AKR1C3), type 1 3α-HSD (AKR1C4), porphobilinogen deaminase (PBGD), glyceraldehyde-3-phosphate dehydrogenase (GAPDH), peroxisome proliferator-activated receptor-γ (PPARγ), prostaglandin (PG), primary epithelial cells (PEC), primary stromal cells (PSC).

ABSTRACT (247 words)

Transcript levels for steroid transforming enzymes that regulate ligand access to the androgen receptor e.g. type 2 5α-reductase, ketosteroid reductases (aldo-keto reductase (AKR)1C1-AKR1C4), the major prostatic oxidative 3α-hydroxysteroid (HSD) retinol dehydrogenase (RODH)-like 3α-HSD (RL-HSD) as well as transcript levels of nuclear receptors [androgen receptor (AR), estrogen receptor (ER)α and ERβ] were measured in whole human prostate and in cultures of primary epithelial cells (PEC) and primary stromal cells (PSC) from normal prostate, prostate adenocarcinoma (CaP) and benign prostatic hyperplasia (BPH) using validated real-time RT-PCR protocols. Normal PEC (n=14) had higher levels of type 2 5α-reductase (2.5-fold), AKR1C1 (10-fold $p<0.001$), AKR1C2 (115-fold $p<0.001$) and AKR1C3 (6-fold $p<0.001$) than normal PSC (n=15). By contrast, normal PSC had higher levels of AR (8-fold $p<0.001$) and RL-HSD (21-fold $p<0.001$) than normal PEC. In CaP PEC (n=14) elevated transcript levels for AKR1C3 (3-fold $p=0.055$) and AR (5-fold $p=0.051$) were indicated, but were not statistically significant. In BPH PSC (n=21) a coordinated increase in transcripts of type 2 5α-reductase (2-fold p=?), AR (2-fold $p<0.001$), AKR1C1 (4-fold $p<0.001$), AKR1C2 (10-fold $p<0.001$), AKR1C3 (4-fold $p<0.001$) and RL-HSD (3-fold $p<0.005$) suggests an increased capacity for androgen signaling. Transcripts for nuclear receptors showed changes in the AR:ERβ ratio and indicates an important regulatory role of ERβ signaling in normal PEC (AR:ERβ ratio 8) as compared to normal PSC (AR:ERβ ratio 280). These findings may provide a mechanistic underpinning as to why BPH is more responsive to androgen ablative therapy than CaP and suggest that targeting non-androgen pathways may be a better therapy for CaP.

INTRODUCTION

The human prostate is essential for normal male reproduction since it excretes the prostatic fluid necessary for the maintenance of sperm (1, 2). The mature gland is regulated by the most potent androgen 5α-dihydrotestosterone (DHT) which is responsible for the maintenance and growth of the prostate (3, 4). Androgen actions are regulated at the pre-receptor level by enzymes responsible for the formation and elimination of DHT e.g. type 2 5α-reductase and the hydroxysteroid dehydrogenases (HSDs). Dysregulation of these enzymes may lead to the development of androgen dependent diseases that include prostate adenocarcinoma (CaP) and benign prostatic hyperplasia (BPH).

Within the normal prostate, DHT is formed from the irreversible reduction of circulating gonadal 17β-hydroxy-androst-4-ene-3-one (testosterone) by type 2 5α-reductase (Figure 1) (3, 4). In contrast, within the prostate of aging males DHT production may depend upon the local production of testosterone from the inactive androgen Δ^4-androstene-3,17-dione (androstenedione) by type 2 3α-HSD/type 5 17β-HSD also known as aldo-keto reductase (AKR) 1C3 (AKR1C3) (5-8). The subsequent reduction of testosterone to DHT by type 2 5α-reductase completes its formation. Intraprostatic levels of DHT are regulated by reductive and oxidative HSDs. AKR1C2 (type 3 3α-HSD and a 3-ketosteroid reductase) eliminates DHT by reducing it to the inactive androgen 5α-androstane-3α,17β-diol (3α-diol) (8-11). By contrast, AKR1C1 (20α-HSD and a 3-ketosteroid reductase) converts DHT to 5α-androstane-3β,17β-diol (3β-diol) (11) a pro-apoptotic ligand for estrogen receptor (ER)β (12-14). The ratio of AKR1C1:AKR1C2 may be important in determining if a pro-apoptotic signal is

generated in the prostate. By contrast a comparison of five candidate oxidative 3α-HSDs revealed that RODH-like 3α-HSD (RL-HSD) was most likely responsible for the oxidation of 3α-diol back to DHT (15).

Identifying the enzymes that regulate the formation of DHT has led to therapeutic advances in treating prostate diseases. For example, the type 2 5α-reductase mechanism-based inactivator, finasteride, reduces intraprostatic levels of DHT by approximately 80% (16-18). However, complete depletion of DHT may never be achieved until the enzymes responsible for its formation and elimination are fully investigated and their expression compared between normal and diseased prostates. Many steroid transforming enzymes involved in androgen signaling in normal versus diseased prostate tissues have been investigated, but in many cases their cell specific expression was never inspected or the enzymes were compared in other species (6, 7, 9, 10, 19-24). Furthermore, their co-localization with the androgen receptor (AR), ERα and ERβ has not been determined (25-27).

We report transcript profiling of proteins associated with androgen signaling in whole human prostate and in normal and diseased (CaP, BPH) prostate primary epithelial cells (PEC) and prostate primary stromal cells (PSC) by real-time RT-PCR. The mRNA expression was determined for steroidhormone receptors (AR, ERα, ERβ) and relevant steroid transforming enzymes e.g. type 2 5α-reductase, the major oxidative 3α-HSD (RL-HSD), other oxidative 3α-HSDs [11-*cis* retinol dehydrogenase (RODH 5), L-3-hydroxyacyl coenzyme A dehydrogenase/type 10 17β-HSD (ERAB), novel type of human microsomal 3α-HSD (NT 3α-HSD) and retinol dehydrogenase 4 (RODH 4)], the 3-, 17-, and 20-ketoreductases [AKR1C1 (20-ketosteroid reductase), AKR1C2 (3-

ketosteroid reductase), AKR1C3 (17-ketosteroid reductase), AKR1C4 (3-ketosteroid reductase)] and cytochrome p450 7B1 (P4507B1). The mRNA expression data indicated that many of the transcripts displayed a celltype-specific expression. In BPH PSC there was an increase in the mRNA transcripts for type 2 5α-reductase, AR, AKR1C1, AKR1C2, AKR1C3 and RL-HSD. In CaP PEC no statistically significant changes were observed, but elevated expression of AKR1C3 and AR was noted. Changes in the expression of nuclear receptors revealed significant differences in the AR:ERβ ratio level. The ratio was uniformly higher in normal PSC (AR:ERβ ratio 280) than in normal PEC (AR:ERβ ratio 8) and the ratio increased 3-fold in BPH PSC (AR:ERβ ratio 820). Our data suggest that estrogen signaling may have an important regulatory function in PEC since the AR:ERβ ratio is suppressed 30-fold compared to PSC. The data explains why androgen ablative therapy is an effective treatment for BPH but not for late-stage CaP.

MATERIALS AND METHODS

Cultured prostate PEC and PSC

The cultured prostate PEC and PSC were maintained as previously reported (10, 28, 29). From these protocols normal (n=14) and diseased (CaP n=14, BPH n=6) prostate PEC and normal (n=15) and diseased (CaP n=16, BPH n=21) prostate PSC were isolated. CaP PEC and PSC were obtained from patients with a Gleason Grade 3+3 to 4+4.

Real-Time PCR

Real-time RT-PCR determined relative transcript levels for different proteins involved in androgen signaling. Total RNA pooled from 32 human Caucasian male prostates was purchased from BD Bioscience (Palo Alto, CA) and 1 μg of total RNA was reverse transcribed using GeneAmp RNA PCR Kit (Applied Biosystems, Foster City, CA). Total RNA from cultured prostate PEC and PSC was isolated as previously reported and 1 μg of RNA was reverse transcribed using GeneAmp RNA PCR Kit. Real-time PCR was performed using a DNA Engine Opticon2 Continuous Fluorescence Detector (MJ Research Incorporation, Waltham, MA).

The real-time PCR method and primers used in this study were previously reported for the oxidative 3α-HSDs (RL-HSD, ERAB, RODH 5, NT 3α-HSD and RODH 4) (15), the ketosteroid reductases (AKR1C1-AKR1C4) (30), type 2 5α-reductase (31), P4507B1 and PBDG (32), AR (33), ERα and ERβ (34) and GAPDH (35). Primer specificity was determined by separating the PCR product on a 3% gel and by sequencing to ensure only the amplification of the desired gene. At the end of the PCR reaction, melting curves were performed for those reactions that utilized SYBR Green (Qiagen Inc,

Valencia, CA) to ensure the specific amplification of the desired product. The RT-PCR method was linear ($r \geq 0.995$) over a dynamic range (10^9) as determined by plotting the $\log_{10}$ fluorescence intensity versus the number of cycles. The conditions for the real-time PCR using SYBR Green were as follows: 95 °C for 15 min followed by 40 cycles of 94 °C for 15 sec, X °C for 30 sec and 72 °C for 30 sec (whereby X = 56 °C for AKR1C4 (with 4% DMSO); 57 °C for AKR1C1; 58 °C for AR, P4507B1, GAPDH and PBGD; 60 °C for RL-HSD, NT 3α-HSD, RODH 4, ERα and ERβ; 61 °C for AKR1C2 and AKR1C3; and 63 °C for ERAB and RODH 5). Type 2 5α-reductase primers used were previously reported (31) except that the TaqMan probe (Applied Biosystems) used was 5' 6FAM dCTC ACT TTG TTT CCT TGG GCT GCG AG TAMRA 3'. The cycles for the TaqMan real-time PCR using TaqMan Universal Mix (Roche Diagnostics, Indianapolis, IN) were as follows: 50 °C for 3 min then 95 °C for 10 min followed by 40 cycles of 94 °C for 15 sec, 60 °C for 60 sec. Full length standards (2,500,000 fg – 0.025 fg) were generated for AKR1C1, AKR1C2, AKR1C3, AKR1C4, ERAB, RL-HSD, RODH 5, NT 3α-HSD and RODH 4 from their appropriate cDNA plasmids (pcDNA3-AKR1C1, pcDNA3-AKR1C2, pcDNA3-AKR1C3, pcDNA3-AKR1C4, pcDNA2-ERAB, pcDNA3-RL-HSD, pcDNA3-RODH 5, pcDNA3-NT 3α-HSD and pcDNA3-RODH 4). Total mRNA isolated from liver (BD Bioscience, Palo Alto, CA) was reverse transcribed to cDNA using GeneAmp RNA PCR Kit and subsequently PCR product standards (2,500,000 fg -0.025 fg) were generated for P4507B1, AR, ERα, ERβ, type 2 5α-reductase, GAPDH and PBGD by isolating the desired PCR product. The product was isolated by gel purification and used as real-time PCR standards with correction factors for GADPH (3.30), PBGD (7.48), AR (11.79), type 2 5α-reductase (7.08), ERα (16.53),

ERβ (11.12) and P4507B1 (10.01) due to the difference in molecular weight between full-length and PCR product standards. Samples (fg) were divided by the total cDNA in each reaction (ng) and subsequently normalized to the relative amount of PBGD and GAPDH, which was calculated to be the individual sample divided by the sample set average and similar patterns were observed.

Statistical analysis of transcripts in normal versus diseased (CaP and BPH) prostate PEC and PSC

The normal and diseased groups were compared using the Mann-Whitney rank sum test by the statistical analysis program Sigma Stat (Port Richmond, CA). This test was selected as the groups were of unequal sizes and assumes that the data followed non-Gaussian distributions. The statistical analysis was performed to compare prostate PEC [normal n=14 and diseased (CaP n=14, BPH n=6)] as well as for prostate PSC [normal n=15 and diseased (CaP n=16, BPH n=21)]. The data was compared across groups and statistical differences were identified by a p value ($p<0.05$) for significance.

RESULTS

Relative expression of mRNA transcripts that regulate androgen signaling in whole human prostate

We determined the relative expression of mRNA transcripts involved in regulating the androgen signal in whole human prostate by real-time RT-PCR. Transcripts included those for nuclear hormone receptors (AR, ERα and ERβ) and those for steroid transforming enzymes: type 2 5α-reductase, the ketosteroid reductases (AKR1C1-AKR1C4), the oxidative 3α-HSDs (RL-HSD, ERAB, RODH 4, RODH 5 and NT 3α-HSD) and P4507B1. AKR1C1, AKR1C2 and AKR1C3 can regulate the androgen signal by increasing the amount of 3β-diol, 3α-diol and testosterone formed, respectively (5, 11). Oxidative 3α-HSDs can oxidize 3α-diol to DHT; of these RL-HSD was identified as the major oxidative 3α-HSD in normal human prostate (15). P4507B1 can also regulate the hormonal signal by converting 3β-diol to 5α-androstane-3β,7α,17β-triol, thus decreasing a pro-apoptotic ligand for ERβ (36, 37). Transcripts were measured in total RNA isolated and pooled from 32 normal whole human prostates. The mRNA expression levels were normalized to the high-copy housekeeping gene GAPDH and the low-copy housekeeping gene PBGD and similar patterns were observed.

The real-time RT-PCR data indicated that the mRNA transcripts of proteins that regulate the androgen signal were expressed in normal human prostate (Figure 2). The mRNA transcripts for type 2 5α-reductase and the AR were much higher than that observed for any of the other genes (by approximately 50-fold). AKR1C1 and ERα were the next most abundantly expressed transcripts, followed by P4507B1, ERAB, RL-HSD, AKR1C2, ERβ and AKR1C3. Finally very low levels of RODH 5, NT 3α-HSD

and RODH 4 were detected. The transcript for AKR1C4 was not detected in normal prostate and confirms previous findings that it is liver-specific (8, 30). AKR1C1 was approximately 13-fold more highly expressed than AKR1C2, suggesting that conversion of DHT to 3β-diol is favored unless this ratio changes in diseased prostate. The data also indicated that the AR was much more highly expressed than ERα (10-fold) and ERβ (66-fold) whereas ERα was approximately 6-fold more highly expressed than ERβ. These results indicated that many of the transcripts for steroid transforming enzymes involved with androgen signaling are expressed in normal human prostate, but did not indicate the cell type specificity or their co-localization with steroid receptors.

Transcripts of proteins that regulate androgen signaling show a cell type-specific expression: comparison of normal prostate PEC with normal prostate PSC

The expression of mRNA transcripts for proteins involved in androgen signaling was determined in normal prostate PEC and PSC cultures. The results indicated a cell type-specific expression of the transcripts (Figure 3A, Table 1). In normal PEC the ketosteroid reductases (AKR1C1-AKR1C3) were most highly expressed. In the same cells, ERAB was the highest expressed followed by NT 3α-HSD, AR, type 2 5α-reductase and P4507B1. Also RODH 5, ERα and ERβ were detected in normal prostate PEC, but at low levels. The expression in normal prostate PSC indicated that AKR1C1 was the highest expressed followed by AR, ERAB, RL-HSD, AKR1C3 and AKR1C2 and to a lesser extent RODH 5 and type 2 5α-reductase. AKR1C4 was not detected in either normal PEC or normal PSC and thus re-confirms previous findings (8, 30).

The ratio for the mRNA expression in normal PEC versus normal PSC indicated that many of the transcripts associated with androgen signaling had a cell type-specific preference (Figure 3B). For example, the mRNA transcript for NT 3α-HSD was only detected in normal PEC and was absent in the normal PSC. The mRNA expression of those transcripts that showed a preferential expression in normal PEC over that seen in normal PSC included NT 3α-HSD (~3000-fold, $p<0.001$), AKR1C2 (~115-fold, $p<0.001$), P4507B1 (~75-fold, $p<0.001$), RODH 4 (~20-fold, $p<0.001$), AKR1C1 (~10-fold, $p<0.001$), AKR1C3 (~6-fold, $p<0.001$), ERAB (~4-fold, $p<0.001$) and ERβ (~4-fold, $p<0.001$) using median values (Figure 3B, Table 1). In contrast, the mRNA expression of those transcripts that showed a preferential expression in normal PSC over that seen in normal PEC included RL-HSD (~20-fold, $p<0.001$) and AR (~8-fold, $p<0.001$) using median values. Type 2 5α-reductase, RODH 5 and ERα were expressed almost equally in both normal PEC and PSC, but a slight preference for normal PEC was noted for type 2 5α-reductase (~2.5-fold, $p=0.121$) and a slight preference for normal PSC was noted for RODH 5 (~1.5-fold, $p=0.198$) and ERα (~1.5-fold, $p=0.121$).

Changes in the expression of mRNA transcripts in diseased (CaP and BPH) PEC and PSC

The expression levels of mRNA transcripts for proteins involved in androgen signaling were compared in normal and diseased PEC and PSC using real-time RT-PCR (Table 1, Figure 4 and Figure 5). As the values were derived from unmatched samples and non-Gaussian distributions were observed we utilized the Mann-Whitney rank sums

test to determine if changes in the expression of transcripts were statistical significant between median values.

Comparisons in mRNA expression in PEC from normal and diseased CaP and BPH tissue indicated that several trends existed. An increase in the expression of AKR1C3 (3-fold $p=0.055$) and AR (5-fold $p=0.051$) is suggested in CaP PEC as compared to normal PEC, although statistical significance was not obtained. The remainder of the steroid transforming enzymes and steroid receptors were not significantly altered in CaP PEC. No significant changes were observed in the expression of transcripts for the steroid transforming enzymes or steroid receptors between BPH and normal PEC. This may not be surprising as BPH is believed to originate in stromal cells of the prostate (McNeal, J. E. Pathology of benign prostatic hyperplasia, Insight into etiology. Urol Clin North Am 17:477, 1990).

In normal and diseased (CaP and BPH) PSC mRNA expression indicated that several trends also existed. A significant increase in expression was observed in CaP PSC as compared to normal PSC for RODH 4 (2-fold $p<0.005$), RODH 5 (2-fold $p<0.05$), ERAB (1.5-fold $p<0.05$), AKR1C1 (2-fold $p<0.05$) and AKR1C3 (2-fold $p=0.060$). The remainder of the steroid transforming enzymes and steroid receptors were unaltered at the transcript level. Major changes in transcript levels of proteins involved in regulating the androgen signal were observed for BPH PSC as compared to normal PSC. These changes suggest an increase in mRNA expression for ERAB (2-fold $p<0.001$), AKR1C1 (4-fold $p<0.001$), AKR1C2 (10-fold $p<0.001$), AKR1C3 (4-fold $p<0.001$), AR (2-fold $p<0.001$), RL-HSD (3-fold $p<0.005$) and to a lesser extent type 2 5α-reductase (2-fold $p=0.072$) and a decrease for ERα (2-fold $p=0.072$). The increase in

transcripts for the oxidative 3α-HSD (RL-HSD) and AR could lead to altered androgen gene transcription in BPH PSC.

Representative scatter box plots for transcripts in normal and diseased PEC and PSC

As the samples were unmatched and did not follow a Gaussian distribution, we plotted all the transcripts investigated in this study as scatter box plots to visually identify potential trends. Representative scattered box plots for type 2 5α-reductase, RL-HSD, AKR1C1, AKR1C2 and AKR1C3 as well as for the nuclear hormone receptors (AR, ERα and ERβ) in normal and diseased (CaP and BPH) PEC and PSC are shown (Figure 4 and Figure 5, respectively). The data indicates that several of the transcripts are more highly expressed in PEC than PSC, but transcripts in PEC were often unaltered in diseases. The data also indicates that several of the transcripts have an elevated expression in BPH PSC, which is in agreement with the statistical analysis. The increased expression in AKR1C3 > AR > RL-HSD > type 2 5α-reductase suggests that these cells have gained steroid transforming enzymes necessary to produce excess DHT. Furthermore, elevated expression of AR can lead to an increase in androgen signaling in BPH PSC. Elevated mRNA expression of AKR1C1 and AKR1C2 was noted and could indicate increase capacity to metabolize DHT in the BPH PSC. The scatter box plots also permit the preferential expression of the transcripts for the indicated proteins to be directly compared since the axes are the same for each individual transcript between normal, CaP and BPH PEC and PSC cells.

Altered ratio of AKR1C1:AKR1C2 and estrogen signaling

In whole prostate the ratio of AKR1C1:AKR1C2 was 13, but was dramatically reduced to 1.9 in normal PEC (Figure 6A). This ratio remained unaltered in CaP and BPH PEC. Thus it is predicted that PEC will produce similar amounts of 3β-diol and 3α-diol irrespective of disease status. By contrast, the ratio of AKR1C1:AKR1C2 was significantly increased in normal PSC (AKR1C1:AKR1C2 ratio 22) as compared to whole prostate (AKR1C1:AKR1C2 ratio 13). This may indicate that normal PSC will generate more 3β-diol than 3α-diol in comparison to PEC. Furthermore, a decrease in the ratio in PSC was noted in CaP (AKR1C1:AKR1C2 ratio 13) and BPH (AKR1C1:AKR1C2 ratio 8) PSC and indicates that the 3β-diol signal will be reduced.

Altered ratio of steroid receptors (AR, ERα and ERβ) in normal and diseased prostate PEC and PSC indicate decreased ER signaling

The ratios of the steroid receptors (AR, ERα and ERβ) were compared in normal and diseased (CaP and BPH) PEC and PSC (Figure 6B and Figure 6C). The data indicated that in normal PEC the mRNA transcript for the AR is more than 6-fold ($p<0.05$) and 8-fold ($p<0.005$) more highly expressed than ERα or ERβ, respectively. ERα and ERβ mRNA transcripts were equally expressed in normal PEC ($p=0.765$).

The ratio between AR:ERα increased from 6 in normal PEC to 30 in CaP PEC ($p<0.005$) and the ratio of AR:ERβ increased from 8 in normal PEC to 50 in CaP PEC ($p<0.001$) and was due to elevated AR expression whereas transcripts for ERα and ERβ were constant. This would suggest that in CaP PEC the androgen signal increases due to an elevated AR.

In BPH PEC the ratio between AR and ER decreased due to a 4-fold decrease in AR while ERα and ERβ levels remains unaltered; however, this decrease did not reach statistical significance (AR:ERα 4 p=0.132 and AR:ERβ 1.6 p=0.485). The ratio between ERα and ERβ mRNA transcripts indicated that ERβ was more highly expressed by 3-fold in BPH PEC. This may suggest that in these cells the estrogen signal is elevated by a decrease in AR and a change in ERβ levels.

In normal PSC, the ratios between AR and ER transcripts were more dramatic. The AR mRNA transcript was expressed approximately 50-fold higher than ERα ($p<0.001$) and 280-fold higher than ERβ ($p<0.001$). This is due to both an increase in mRNA transcript for the AR, which was 10-fold higher in the normal PSC as compared to normal PEC and by a 4-fold decrease in ERβ. This suggests that androgen signaling is more important in normal PSC than in normal PEC while the estrogen signal is more important in normal PEC than in normal PSC. The transcript level for ERα indicated that it was 5-fold higher than ERβ in normal PSC ($p<0.001$) suggesting that estrogen signaling may be through ERα, which is in agreement with previous publications (38, 39).

The ratio between AR:ERα in CaP PSC increased to greater than 60 as compared to 50 for normal PSC and the ratio between AR:ERβ in CaP PSC remained the same (AR:ERβ ratio 275) as compared to normal PSC (AR:ERβ ratio 280). The ratio between ERα and ERβ mRNA transcripts decreased slightly in CaP PSC (AR:ERβ ratio 4 $p<0.001$).

The ratio between AR:ERα in BPH PSC increased to 180 compared to 50 for normal PSC and the ratio between AR:ERβ in BPH PSC increased to 820 as compared to

280 for normal PSC. The ratio between ERα and ERβ mRNA transcripts decreased slightly in BPH PSC (ERα:ERβ ratio 4.5 $p<0.01$) as compared to normal PSC as the expression of both ERα and ERβ decreased by approximately 2-fold. This may suggest that in BPH PSC androgen signaling is dramatically increased due to an increase in AR expression and a concomitant decrease in ER expression.

DISCUSSION

We have investigated the expression of transcripts involved in androgen signaling by real-time RT-PCR in normal whole human prostate and in normal and diseased (CaP and BPH) cultured prostatic epithelial and stromal cells (PEC and PSC).In considering our results, it should be kept in mind that cultured PEC have a phenoptype similar to basal and/or transit amplifying cells (Peehl Endocrine-Related Cancer 12:19-47, 2005), and cultured PSC are fibroblastic and/or smooth muscle (Peehl Prostate 45:115-123, 2000). Thus, androgen signaling of differentiated secretory epithelial cells is not addressed in our study.

Transcript levels were measured using total RNA from 32 pooled whole human prostates. The tissue contained all the necessary transcripts to modulate the androgen signal. Type 2 5α-reductase and AR mRNA were the highest expressed in normal prostate. Furthermore, the mRNA expression from normal prostate indicated that the major oxidative 3α-HSD (RL-HSD) was also present. Consequently, within the normal prostate there are steroid transforming enzymes present that can activate the androgen signal either by reducing testosterone to DHT (type 2 5α-reductase) or by oxidizing 3α-diol back to DHT (RL-HSD) (15). The ketosteroid reductases (AKR1C1-AKR1C3) were expressed in whole human prostate. It is believed that AKR1C1 and AKR1C2 may be involved in the metabolism of DHT to 3β-diol or 3α-diol, respectively, while AKR1C3 reduces androstenedione to testosterone (5, 11). AKR1C1 was the dominant AKR1C isoform expressed and may be a growth constraint in normal prostate as 3β-diol is a pro-apoptotic ligand for the ERβ. Expression profiles of AR, ERα and ERβ in whole normal

prostate indicated that androgen signaling dominated as the mRNA transcript for the AR was more than 10-fold and 66-fold higher expressed than ERα and ERβ, respectively.

The expression of transcripts that control androgen signaling in normal PEC and PSC indicated that they displayed a cell-type-specific preference. In normal prostate PEC, AKR1C isozymes were the highest expressed followed by ERAB, type 2 5α-reductase, AR and P4507B1. The ratio of AR to ER (ERα and ERβ) indicated that the AR was more highly expressed by 8-fold. This finding leads to the following model of androgen signaling in normal PEC (Figure 7). Δ^4-Androstenedione is reduced by AKR1C3 to yield testosterone, which is subsequently reduced by type 2 5α-reductase to yield DHT. DHT can activate the androgen signal by binding to the AR. Two additional fates exist for DHT - it can be converted to 3β-diol by AKR1C1 to activate ERβ or it can be converted to the inactive androgen 3α-diol by AKR1C2. Furthermore, P4507B1 could eliminate 3β-diol by metabolizing it to 5α-androstane-3β,7α,17β-triol that is excreted. The data suggests that estrogen signaling by 3β-diol has a more important regulatory growth function in epithelial cells than stromal cells due to the ratio of AR:ERβ (8 in PEC as compared to 280 in PSC). This is substantiated by both the ERβ-KO mouse and the P4507B1-KO mouse (12, 37). ERβ-KO mice had increased hyperplastic foci in the epithelial cells of the prostate which were identified as low grade prostatic intraepithelial neoplasia (PIN) as compared to wild-type mice (12, 40). The hyperplasia was reduced in the wild-type mice with 3β-diol, but was unaltered in the ERβ-KO mice. Also, P4507B1-KO mice displayed hypo-proliferative prostates as compared to wild-type mice (37). As ERβ signaling leads to an increase in apoptosis of epithelial cells of the prostate and P4507B1 regulates the local concentration of 3β-diol, a

ligand for the ERβ (12, 13, 40-42), these results indicate the importance of both the estrogen signal and the pro-apoptotic ligand 3β-diol in regulating the normal growth of prostatic epithelial cells.

In normal PSC, the AKR1C isozymes were highly expressed, albeit 10-fold less than in normal PEC. Also detected in normal PSC were type 2 5α-reductase, AR and RL-HSD. In these cells the expression of AKR1C3 was still 6-fold greater than type 2 5α-reductase. However, the ratio of AR to ER dramatically favored androgen signaling as the AR was 50-fold higher than ERα and 280-fold higher than ERβ. Moreover, AR was 8-fold higher in the normal PSC as compared to the normal PEC. This leads to the following model of androgen signaling in normal PSC (Figure 7). Δ^4-Androstenedione is reduced by AKR1C3 to yield testosterone, which is subsequently reduced by type 2 5α-reductase to yield DHT. An additional source of DHT is available via RL-HSD which will oxidize 3α-diol back to DHT. DHT can be eliminated by being reduced to 3β-diol or 3α-diol by AKR1C1 and AKR1C2, respectively. The cells are highly responsive to androgens due to high AR expressed and the favorable ratio of AR:ERβ.

The mRNA expression of transcripts involved in androgen signaling was investigated in normal and diseased PEC. In CaP PEC a trend indicates a potential increase in AKR1C3 and AR compared to normal PEC. In addition the ratio of AR:ERα increases in these cells as compared to the normal PEC. These changes would support an increase in androgen signaling via prostatic testosterone and the AR (Figure 7). Dramatic differences in transcripts may be lost unless the stage of the disease is considered. Thus although 14 samples were examined in the present study, more samples may have to be stratified by Gleason score to confirm that the observed trend holds. It will also be

important to determine if similar trends exist with CaP of lower Gleason grades. Our data show a slight trend in the increase of AKR1C2 in CaP PEC. This would be consistent with our previous report which showed up-regulation of AKR1C2 in epithelial cells from CaP patients (10). The data would be inconsistent with the down-regulation of AKR1C2 noted by real-time RT-PCR in whole CaP tissue versus adjacent normal tissue (9). The difference may be related to the fact that discrete differences in cell type may be masked when whole sections are examined.

In BPH PEC a trend indicates a potential increase in the ERβ signal due to a decrease in the expression of AR and an increase in AKR1C1 as compared to normal PEC but other changes were not evident. This would suggest that androgen signaling may be decreased as compared to normal PEC due to a decrease in AR expression and a concomitant increase in AKR1C1 leading to an increase in 3β-diol (Figure 7). In BPH, proliferative properties of epithelial cells appear to be dependent upon growth factors other than androgens, thus changes in transcripts for steroid transforming enzymes and steroid receptors involved in androgen signaling were not expected (43-45).

In CaP PSC increases in ERAB, RODH 5, RODH 4 and AKR1C1 as compared to normal PSC were noted. ERAB, RODH 5 and RODH 4 have been implicated in the oxidation of 3α-diol back to DHT. ERAB is not an efficient enzyme at this reaction when compared to RL-HSD which is unchanged in expression level (15). RODH 5 and RODH 4 may be either involved in producing more DHT or their elevated expression is required for other functions. RODH5 and RODH 4 may be involved in regulating ligands for RXR and RAR and may be anti-proliferative when the liganded receptor heterodimerizes with peroxisome proliferator-activated receptor (PPAR)γ. In addition

AKR1C1 produces 3β-diol, a pro-apoptotic ligand. Together these combined signals may favor inhibition of stromal cell growth in CaP.

In BPH PSC some of the most dramatic differences were observed. There was a coordinated increase in ERAB, AKR1C1, AKR1C2, AKR1C3, RL-HSD, AR and, to a lesser extent type, 2 5α-reductase. In addition the ratio of AR:ERβ which is 280 in normal PSC increases further in BPH PSC to greater than 820. These changes would support an increase in androgen signaling via DHT not only by the reduction of testosterone by type 2 5α-reductase but also by the oxidation of 3α-diol by RL-HSD (Figure 7). Elevated AKR1C3 expression would produce more prostatic testosterone, and elevated AKR1C1 and AKR1C2 would provide a mechanism for the clearance of excess androgen. When combined these data support the concept that BPH PSC have become more androgenic than normal PSC.

Stromal-epithelial interactions of the prostate are important in maintaining the morphology and coordinating the growth of each cell type (43-45). The inactive androgen, 3β-diol, may regulate stromal-epithelial interactions by binding to ERβ and inducing apoptosis. Recent experiments have indicated the important regulatory role of 3β-diol and ERβ signaling; however, these experiments are unable to indicate whether 3β-diol is formed locally within epithelial cells or within stromal cells to act in a paracrine manner on epithelial cells. Furthermore, it is also possible that within stromal cells the 3β-diol produced may activate stromal ERβ signaling and thus regulate the growth of epithelial cells through stromal-epithelial interactions (e.g. through growth factors). The ratios of AKR1C1:AKR1C2 may play an important role in regulating normal prostate growth by altering the amount of 3β-diol produced. Examination of

these ratios indicated that epithelial cells (AKR1C1:AKR1C2 ratio 2 in PEC) would produce less 3β-diol than stromal cells (AKR1C1:AKR1C2 ratio 22 in PSC), indicating that either 3β-diol regulates the growth of epithelial cells in a paracrine manner or through stromal ERβ signaling. The AKR1C1:AKR1C2 ratio decreases in CaP and BPH PSC as compared to normal PSC, suggesting that in these cells there is a decrease in the amount of 3β-diol that can activate ERβ signaling. The binding efficiency of 3β-diol is approximately 10-fold less than 17β-estradiol for ERβ; however, within the prostate 3β-diol levels are approximately 100-fold higher, suggesting that 3β-diol would be the favored ligand for ERβ (40). As a result of a decrease in the AKR1C1:ARK1C2 ratio in diseased prostates as compared to normal PSC it could be predicted that 3β-diol levels would decrease, thus losing the growth constraint seen with 3β-diol and ERβ signaling.

In summary, we have measured levels of transcripts that regulate androgen signaling in normal prostate, and epithelial and stromal cells cultured from normal prostate, BPH and CaP. We noted that the processing of the androgen signal may differ based on cell-type and prostate disease. Our data suggest that estrogen signaling may be an important regulatory function in epithelial cells as compared to stromal cells due to lower AR:ERβ ratios and may explain why androgen ablative therapy is more effective for BPH. The data also suggests why androgen ablative therapy is not effective in treating late stage CaP and treatments that target non-androgen pathways (e.g. targeting ERβ with a selective estrogen receptor modulator) may be a better therapy for CaP.

ACKNOWLEDGMENTS

We would like to thank S. Bruce Malkowicz, Department of Urology, University of Pennsylvania School of Medicine, Philadelphia, PA, for discussion of the manuscript.

REFERENCECES

1. Hayward, S. W. and Cunha, G. R. The prostate: development and physiology. Radiol Clin North Am, *38:* 1-14, 2000.
2. Wilson, J. D., Leihy, M. W., Shaw, G., and Renfree, M. B. Androgen physiology: unsolved problems at the millennium. Mol Cell Endocrinol, *198:* 1-5, 2002.
3. Andersson, S., Berman, D. M., Jenkins, E. P., and Russell, D. W. Deletion of steroid 5 alpha-reductase 2 gene in male pseudohermaphroditism. Nature, *354:* 159-161, 1991.
4. Russell, D. W. and Wilson, J. D. Steroid 5 alpha-reductase: two genes/two enzymes. Annu Rev Biochem, *63:* 25-61, 1994.
5. Pelletier, G., Luu-The, V., El-Alfy, M., Li, S., and Labrie, F. Immunoelectron microscopic localization of 3beta-hydroxysteroid dehydrogenase and type 5 17beta-hydroxysteroid dehydrogenase in the human prostate and mammary gland. J Mol Endocrinol, *26:* 11-19, 2001.
6. Lin, H. K., Steckelbroeck, S., Fung, K. M., Jones, A. N., and Penning, T. M. Characterization of a monoclonal antibody for human aldo-keto reductase AKR1C3 (type 2 3alpha-hydroxysteroid dehydrogenase/type 5 17beta-hydroxysteroid dehydrogenase); immunohistochemical detection in breast and prostate. Steroids, *69:* 795-801, 2004.
7. Dufort, I., Rheault, P., Huang, X. F., Soucy, P., and Luu-The, V. Characteristics of a highly labile human type 5 17beta-hydroxysteroid dehydrogenase. Endocrinology, *140:* 568-574, 1999.

8. Penning, T. M., Burczynski, M. E., Jez, J. M., Hung, C. F., Lin, H. K., Ma, H., Moore, M., Palackal, N., and Ratnam, K. Human 3alpha-hydroxysteroid dehydrogenase isoforms (AKR1C1-AKR1C4) of the aldo-keto reductase superfamily: functional plasticity and tissue distribution reveals roles in the inactivation and formation of male and female sex hormones. Biochem J, *351:* 67-77, 2000.

9. Ji, Q., Chang, L., VanDenBerg, D., Stanczyk, F. Z., and Stolz, A. Selective reduction of AKR1C2 in prostate cancer and its role in DHT metabolism. Prostate, *54:* 275-289, 2003.

10. Rizner, T. L., Lin, H. K., Peehl, D. M., Steckelbroeck, S., Bauman, D. R., and Penning, T. M. Human type 3 3alpha-hydroxysteroid dehydrogenase (aldo-keto reductase 1C2) and androgen metabolism in prostate cells. Endocrinology, *144:* 2922-2932, 2003.

11. Steckelbroeck, S., Jin, Y., Gopishetty, S., Oyesanmi, B., and Penning, T. M. Human cytosolic 3alpha-hydroxysteroid dehydrogenases of the aldo-keto reductase superfamily display significant 3beta-hydroxysteroid dehydrogenase activity: implications for steroid hormone metabolism and action. J Biol Chem, *279:* 10784-10795, 2004.

12. Weihua, Z., Makela, S., Andersson, L. C., Salmi, S., Saji, S., Webster, J. I., Jensen, E. V., Nilsson, S., Warner, M., and Gustafsson, J. A. A role for estrogen receptor beta in the regulation of growth of the ventral prostate. Proc Natl Acad Sci U S A, *98:* 6330-6335, 2001.

13. Guerini, V., Sau, D., Scaccianoce, E., Rusmini, P., Ciana, P., Maggi, A., Martini, P. G., Katzenellenbogen, B. S., Martini, L., Motta, M., and Poletti, A. The androgen derivative 5alpha-androstane-3beta,17beta-diol inhibits prostate cancer cell migration through activation of the estrogen receptor beta subtype. Cancer Res, *65:* 5445-5453, 2005.

14. Cheng, J., Lee, E. J., Madison, L. D., and Lazennec, G. Expression of estrogen receptor beta in prostate carcinoma cells inhibits invasion and proliferation and triggers apoptosis. FEBS Lett, *566:* 169-172, 2004.

15. Bauman, D. R., Steckelbroeck, S., Williams, M. V., Peehl, D. M., and Penning, T. M. Identification of the major oxidative 3alpha-hydroxysteroid dehydrogenase in human prostate that converts 5alpha-androstane-3alpha,17beta-diol to 5alpha-dihydrotestosterone: A potential therapeutic target for androgen dependent disease. Mol Endocrinol, 2006.

16. Uygur, M. C., Arik, A. I., Altug, U., and Erol, D. Effects of the 5 alpha-reductase inhibitor finasteride on serum levels of gonadal, adrenal, and hypophyseal hormones and its clinical significance: a prospective clinical study. Steroids, *63:* 208-213, 1998.

17. McConnell, J. D., Bruskewitz, R., Walsh, P., Andriole, G., Lieber, M., Holtgrewe, H. L., Albertsen, P., Roehrborn, C. G., Nickel, J. C., Wang, D. Z., Taylor, A. M., and Waldstreicher, J. The effect of finasteride on the risk of acute urinary retention and the need for surgical treatment among men with benign prostatic hyperplasia. Finasteride Long-Term Efficacy and Safety Study Group. N Engl J Med, *338:* 557-563, 1998.

18. Andriole, G., Bruchovsky, N., Chung, L. W., Matsumoto, A. M., Rittmaster, R., Roehrborn, C., Russell, D., and Tindall, D. Dihydrotestosterone and the prostate: the scientific rationale for 5alpha-reductase inhibitors in the treatment of benign prostatic hyperplasia. J Urol, *172:* 1399-1403, 2004.

19. Pelletier, G., Luu-The, V., Li, S., Ouellet, J., and Labrie, F. Cellular localization of mRNA expression of enzymes involved in the formation and inactivation of hormonal steroids in the mouse prostate. J Histochem Cytochem, *52:* 1351-1356, 2004.

20. El-Alfy, M., Luu-The, V., Huang, X. F., Berger, L., Labrie, F., and Pelletier, G. Localization of type 5 17beta-hydroxysteroid dehydrogenase, 3beta-hydroxysteroid dehydrogenase, and androgen receptor in the human prostate by in situ hybridization and immunocytochemistry. Endocrinology, *140:* 1481-1491, 1999.

21. Habib, F. K., Ross, M., Bayne, C. W., Bollina, P., Grigor, K., and Chapman, K. The loss of 5alpha-reductase type I and type II mRNA expression in metastatic prostate cancer to bone and lymph node metastasis. Clin Cancer Res, *9:* 1815-1819, 2003.

22. Habib, F. K., Ross, M., Bayne, C. W., Grigor, K., Buck, A. C., Bollina, P., and Chapman, K. The localisation and expression of 5 alpha-reductase types I and II mRNAs in human hyperplastic prostate and in prostate primary cultures. J Endocrinol, *156:* 509-517, 1998.

23. Luo, J., Dunn, T. A., Ewing, C. M., Walsh, P. C., and Isaacs, W. B. Decreased gene expression of steroid 5 alpha-reductase 2 in human prostate cancer:

implications for finasteride therapy of prostate carcinoma. Prostate, *57:* 134-139, 2003.

24. Thomas, L. N., Lazier, C. B., Gupta, R., Norman, R. W., Troyer, D. A., O'Brien, S. P., and Rittmaster, R. S. Differential alterations in 5alpha-reductase type 1 and type 2 levels during development and progression of prostate cancer. Prostate, *63:* 231-239, 2005.

25. Latil, A., Bieche, I., Vidaud, D., Lidereau, R., Berthon, P., Cussenot, O., and Vidaud, M. Evaluation of androgen, estrogen (ER alpha and ER beta), and progesterone receptor expression in human prostate cancer by real-time quantitative reverse transcription-polymerase chain reaction assays. Cancer Res, *61:* 1919-1926, 2001.

26. Linja, M. J. and Visakorpi, T. Alterations of androgen receptor in prostate cancer. J Steroid Biochem Mol Biol, *92:* 255-264, 2004.

27. Gelmann, E. P. Molecular biology of the androgen receptor. J Clin Oncol, *20:* 3001-3015, 2002.

28. Peehl, D. M. Culture of human prostate epithelial cells, p. 159-180. New York: Wiley & Sons, 1992.

29. Peehl, D. M. and Sellers, R. G. Cultured stromal cells: an in vitro model of prostatic mesenchymal biology. Prostate, *45:* 115-123, 2000.

30. Steckelbroeck, S., Bauman, D. R., Ludwig, M., and Penning, T. M. Expression of nonsteroidal anti-inflammatory drug (NSAID) targets in human lung tumor vs. normal tissue: real-time RT-PCR analyses of the expression levels of the aldo-

keto reductases AKR1C1-1C4 and the cyclooxygenases COX-1 and COX-2. in preparation, 2005.

31. Petroni, A., Cappa, M., Blasevich, M., Solinas, M., and Uziel, G. New findings on X-linked Adrenoleukodystrophy: 5alpha-reductase isoform 2 relative gene expression is modified in affected fibroblasts. Neurosci Lett, *367:* 269-272, 2004.

32. Steckelbroeck, S., Watzka, M., Lutjohann, D., Makiola, P., Nassen, A., Hans, V. H., Clusmann, H., Reissinger, A., Ludwig, M., Siekmann, L., and Klingmuller, D. Characterization of the dehydroepiandrosterone (DHEA) metabolism via oxysterol 7alpha-hydroxylase and 17-ketosteroid reductase activity in the human brain. J Neurochem, *83:* 713-726, 2002.

33. Sinha-Hikim, I., Taylor, W. E., Gonzalez-Cadavid, N. F., Zheng, W., and Bhasin, S. Androgen receptor in human skeletal muscle and cultured muscle satellite cells: up-regulation by androgen treatment. J Clin Endocrinol Metab, *89:* 5245-5255, 2004.

34. Bieche, I., Parfait, B., Laurendeau, I., Girault, I., Vidaud, M., and Lidereau, R. Quantification of estrogen receptor alpha and beta expression in sporadic breast cancer. Oncogene, *20:* 8109-8115, 2001.

35. Steckelbroeck, S., Watzka, M., Reissinger, A., Wegener-Toper, P., Bidlingmaier, F., Bliesener, N., Hans, V. H., Clusmann, H., Ludwig, M., Siekmann, L., and Klingmuller, D. Characterisation of estrogenic 17beta-hydroxysteroid dehydrogenase (17beta-HSD) activity in the human brain. J Steroid Biochem Mol Biol, *86:* 79-92, 2003.

36. Martin, C., Ross, M., Chapman, K. E., Andrew, R., Bollina, P., Seckl, J. R., and Habib, F. K. CYP7B generates a selective estrogen receptor beta agonist in human prostate. J Clin Endocrinol Metab, *89:* 2928-2935, 2004.

37. Weihua, Z., Lathe, R., Warner, M., and Gustafsson, J. A. An endocrine pathway in the prostate, ERbeta, AR, 5alpha-androstane-3beta,17beta-diol, and CYP7B1, regulates prostate growth. Proc Natl Acad Sci U S A, *99:* 13589-13594, 2002.

38. Risbridger, G., Wang, H., Young, P., Kurita, T., Wang, Y. Z., Lubahn, D., Gustafsson, J. A., and Cunha, G. Evidence that epithelial and mesenchymal estrogen receptor-alpha mediates effects of estrogen on prostatic epithelium. Dev Biol, *229:* 432-442, 2001.

39. Omoto, Y., Imamov, O., Warner, M., and Gustafsson, J. A. Estrogen receptor alpha and imprinting of the neonatal mouse ventral prostate by estrogen. Proc Natl Acad Sci U S A, *102:* 1484-1489, 2005.

40. Weihua, Z., Warner, M., and Gustafsson, J. A. Estrogen receptor beta in the prostate. Mol Cell Endocrinol, *193:* 1-5, 2002.

41. Thieulant, M. L., Benie, T., and Jouan, P. Ontogeny of 5 alpha-androstan-3 beta, 17beta-diol and 17 beta-estradiol binding to cytoplasm and nuclei of the male rat. Endocrinology, *110:* 1300-1307, 1982.

42. Thieulant, M. L., Benie, T., Michaud, S., Klein, H., and Vessieres, A. Binding and effects of 5 alpha-androstane-3 beta,17 beta-diol in the male rat pituitary. J Steroid Biochem, *19:* 241-246, 1983.

43. Lee, C. Role of androgen in prostate growth and regression: stromal-epithelial interaction. Prostate Suppl, *6:* 52-56, 1996.

44. Wong, Y. C. and Wang, Y. Z. Growth factors and epithelial-stromal interactions in prostate cancer development. Int Rev Cytol, *199:* 65-116, 2000.

45. Cunha, G. R., Hayward, S. W., Wang, Y. Z., and Ricke, W. A. Role of the stromal microenvironment in carcinogenesis of the prostate. Int J Cancer, *107:* 1-10, 2003.

Table 1. Transcript levels in primary cultures of prostate epithelial and stromal cells

Enzyme	Normal PEC*	CaP PEC*	BPH PEC*	Normal PSC*	CaP PSC*	BPH PSC*
ERAB	2.44E-1 {†} (1.31E-1), [2.85E-1]	2.48E-1 (1.93E-1), [3.81E-1]	2.98E-1 (2.58E-1), [3.82E-1]	6.86E-2 (5.47E-2), [9.97E-2]	1.11E-1 {††} (8.78E-2), [1.31E-1]	1.52E-1 {‡} (1.26E-1), [1.79E-1]
RL-HSD	7.54E-4 {†} (1.96E-4), [1.19E-3]	5.08E-4 (2.62E-4), [8.27E-4]	6.48E-4 (3.97E-4), [8.99E-4]	1.46E-2 (7.32E-3), [2.42E-2]	1.48E-2 (4.78E-3), [2.89E-2]	4.44E-2 {§} (2.27E-2), [6.72E-2]
RODH 5	2.71E-3 {†} (7.06E-4), [4.81E-3]	2.16E-3 (1.62E-3), [4.40E-3]	4.93E-3 (1.63E-3), [6.48E-3]	3.30E-3 (2.41E-3), [8.87E-3]	7.44 E-3 {††} (4.83E-3), [1.12E-2]	4.29E-3 (2.66E-3), [6.29E-3]
NT 3α-HSD	1.74E-2 {†} (1.41E-2), [3.44E-2]	2.25E-2 (7.88E-3), [2.80E-2]	3.35E-2 (2.43E-2), [5.63E-2]	5.68E-6 (0.00), [6.86E-5]	2.85E-6 (0.00), [1.66E-5]	0.00 (0.00), [8.10E-6]
RODH 4	5.89E-4 {†} (4.09E-4), [9.29E-4]	4.06E-4 (3.29E-4), [6.41E-4]	5.11E-4 (4.86E-4), [2.01E-3]	2.86E-5 (1.56E-5), [4.89E-5]	6.20E-5 {§} (4.22E-5), [1.17E-4]	9.87E-5 (6.31E-5), [1.48E-4]
5α-R2	8.57E-3 (2.49E-3), [2.02E-2]	1.10E-2 (6.03E-3), [2.16E-2]	2.10E-2 (5.01E-3), [7.51E-3]	3.38E-3 (8.99E-4), [1.18E-2]	4.11E-3 (1.55E-3), [9.13E-3]	6.51E-3 (4.35E-3), [1.40E-2]
P4507B1	5.90E-3 {†} (3.80E-3), [8.08E-3]	4.23E-3 (2.74E-3), [6.61E-3]	7.27E-3 (6.03E-3), [9.35E-3]	7.63E-5 (1.28E-5), [2.45E-4]	8.80E-5 (6.20E-5), [1.71E-4]	1.85E-4 (1.07E-4), [3.61E-4]

Enzyme	Normal PEC*	CaP PEC*	BPH PEC*	Normal PSC*	CaP PSC*	BPH PSC*
AKR1C1	1.360 {†} (6.26E-1), [2.262]	2.218 (1.416), [3.030]	2.388 (2.095), [2.890]	1.32E-1 (8.81E-2), [2.52E-1]	2.26E-1 {††} (1.58E-1), [3.34E-1]	5.45E-1 {‡} (3.49E-1), [1.381]
AKR1C2	6.99E-1 {†} (3.64E-1), [1.287]	1.146 (6.81E-1), [1.724]	1.187 (1.096), [1.449]	6.04E-3 (5.19E-3), [2.59E-2]	1.69E-2 (1.26E-2), [2.41E-2]	6.20E-2 {‡} (2.84E-2), [1.03E-1]
AKR1C3	1.17E-1 {†} (7.84E-2), [3.08E-1]	3.13E-1 (1.65E-1), [6.63E-1]	3.32E-1 (2.42E-1), [7.07E-1]	1.97E-2 (1.42E-2), [4.72E-2]	3.83E-2 (2.94E-2), [4.56E-2]	8.26E-2 {‡} (6.16E-2), [1.32E-1]
AKR1C4	0.000 (0.000), [0.000]	0.000 (0.000), [0.000]	0.000 (0.000), [0.000]	0.000 (0.000), [0.000]	0.000 (0.000), [0.000]	0.000 (0.000), [0.000]
AR	9.49E-3 {†} (2.54E-3), [3.63E-2]	5.19E-2 (3.53E-2), [6.33E-2]	2.23E-3 (7.12E-4), [3.89E-3]	7.77E-2 (5.70E-2), [1.29E-1]	1.11E-1 (8.78E-2), [1.59E-1]	1.45E-1 {‡} (1.30E-1), [1.97E-1]
ERα	1.51E-3 (2.63E-4), [4.70E-3]	1.72E-3 (1.34E-3), [3.89E-3]	5.31E-4 (3.12E-4), [2.02E-4]	1.59E-3 (7.65E-4), [3.57E-3]	1.77E-3 (9.36E-4), [3.49E-3]	8.12E-4 (3.09E-4), [1.77E-3]
ERβ	1.16E-3 {†} (9.45E-4), [1.49E-3]	1.02E-3 (8.08E-4), [1.67E-3]	1.37E-3 (5.24E-4), [1.67E-3]	2.76E-4 (1.78E-4), [4.99E-4]	4.06E-4 (2.10E-4), [5.87E-4]	1.77E-4 (1.29E-4), [4.14E-4]

*The data performed in triplicate represents the median with the 25% deviation in parentheses ( ) and the 75% deviation in block parentheses [ ] are shown with statistically significant differences indicated. Normal (n=14) and diseased (CaP n=14, BPH n=6) prostate PEC and normal (n=15) and diseased (CaP n=16, BPH n=21) prostate PSC were used for the study. Type 2 5α-reductase (5α-R2).

†p value ($p<0.001$) of statistical significance between normal prostate PEC and normal prostate PSC in {}.

‡p value ($p<0.001$) of statistical significance between the normal cell type and indicated diseased cell type in {}.

§p value ($p<0.005$) of statistical significance between the normal cell type and indicated diseased cell type in {}.

††p value ($p<0.05$) of statistical significance between the normal cell type and indicated diseased cell type in {}.

FIGURE LEGENDS

Fig. 1. Androgen metabolism and hormone signaling in human prostate. 5α-Dihydrotestosterone (DHT), 5α-androstane-3α,17β-diol (3α-diol), 5α-androstane-3β,17β-diol (3β-diol), Δ^4-androstene-3,17-dione (androstenedione), 17β-hydroxy-androst-4-ene-3-one (testosterone), hydroxysteroid dehydrogenase (HSD), 3β-HSD/ketosteroid isomerase (KSI), aldo-keto reductase (AKR), 20α-HSD (AKR1C1), type 3 3α-hydroxysteroid dehydrogenase (AKR1C2), type 2 3α-hydroxysteroid dehydrogenase (AKR1C3) and RODH-like 3α-HSD (RL-HSD).

Fig. 2. Relative expression of transcripts involved in androgen signaling in the prostate normalized to PBDG as determined by real-time PCR. One μg of total RNA was reverse-transcribed to cDNA from the prostate and 12.5 ng of cDNA was added to each real-time PCR experiment that was performed in triplicate with the mean shown. Data is normalized to the housekeeping gene PBGD and is represented as expressed fg of each transcript per ng of total cDNA. RODH 5 (R5), RODH 4 (R4) AKR1C1 (1C1), AKR1C2 (1C2), AKR1C3 (1C3), AKR1C4 (1C4), type 2 5α-reductase (5αR2), cytochrome P450 7B1 (7B1).

Fig. 3. Levels of transcripts involved in androgen signaling in normal PEC and PSC as determined by real-time RT-PCR normalized to PBDG. A. Absolute levels and B. epithelial-stromal cell ratios are indicated. A. One μg of total RNA from normal PEC (n=14) and normal PSC (n=15) were reverse-transcribed to cDNA and 50 ng of cDNA was added to each real-time PCR experiment that was performed in triplicate with the

median shown. B. Ratio of the expression of transcripts involved in androgen signaling in normal PEC versus normal PSC demonstrates cell-type-specific expression. Positive values represent higher expression in normal PEC while negative values represent higher expression in normal PSC. *Indicates statistically different expression between PEC and PSC with p values ($p<0.001$) for significance. RL-HSD (rlHSD), RODH 5 (R5), NT 3α-HSD (ntHSD), RODH 4 (R4), AKR1C1 (1C1), AKR1C2 (1C2), AKR1C3 (1C3), AKR1C4 (1C4), type 2 5α-reductase (5αR2), cytochrome P450 7B1 (7B1).

Fig. 4. Representative scatter box plots of enzymes that regulate the ligand access to the AR in normal and diseased (CaP and BPH) PEC and PSC using real-time RT-PCR. One μg of total RNA was reverse-transcribed to cDNA from the PEC and PSC and 50 ng of cDNA was added to each real-time PCR experiment that was performed in triplicate with the mean shown for each sample. Data is normalized to the housekeeping gene PBGD and is represented as expressed fg of each protein per ng of total cDNA. Normal (n=14), CaP (n=14) and BPH (n=6) PEC and normal (n=15), CaP (n=16) and BPH (n=21) PSC were used for the study.

Fig. 5. Representative scatter box plots of nuclear hormone receptors in normal and diseased (CaP and BPH) PEC and PSC using real-time RT-PCR. One μg of total RNA was reverse-transcribed to cDNA from the PEC and PSC and 50 ng of cDNA was added to each real-time PCR experiment that was performed in triplicate with the mean shown for each sample. Data is normalized to the housekeeping gene PBGD and is represented

as expressed fg of each protein per ng of total cDNA. Normal (n=14), CaP (n=14) and BPH (n=6) PEC and normal (n=15), CaP (n=16) and BPH (n=21) PSC were used for the study.

Fig. 6. Ratios of transcripts altering ERβ signaling. Ratio of A. AKR1C1:AKR1C2, B. AR:ERα and C. AR:ERβ in normal and diseased prostates. Normal (n=14), CaP (n=14) and BPH (n=6) PEC and normal (n=15), CaP (n=16) and BPH (n=21) PSC were used for the study. Prostate adenocarcinoma (CaP), benign prostatic hyperplasia (BPH), primary epithelial cells (PEC), primary stromal cells (PSC). Data taken from Table 1.

Fig. 7. Summary of androgen signaling in normal PEC and PSC. A. Androgen signaling in normal PEC with the differences in expression indicated for CaP PEC and BPH PEC as determined by real-time RT-PCR. The ratio between AR and ERβ is indicated in parenthesis. B. Androgen signaling in normal PSC with the differences in expression indicated for CaP PSC and BPH PSC as determined by real-time RT-PCR. The ratio between AR and ERβ is indicated in parenthesis. Androstenedione (AD), testosterone (T), dihydrotestosterone (DHT), 5α-androstane-3α,17β-diol (3α-diol), 5α-androstane-3β,17β-diol (3β-diol), 5α-androstane-3β,7α,17β-diol (triol).

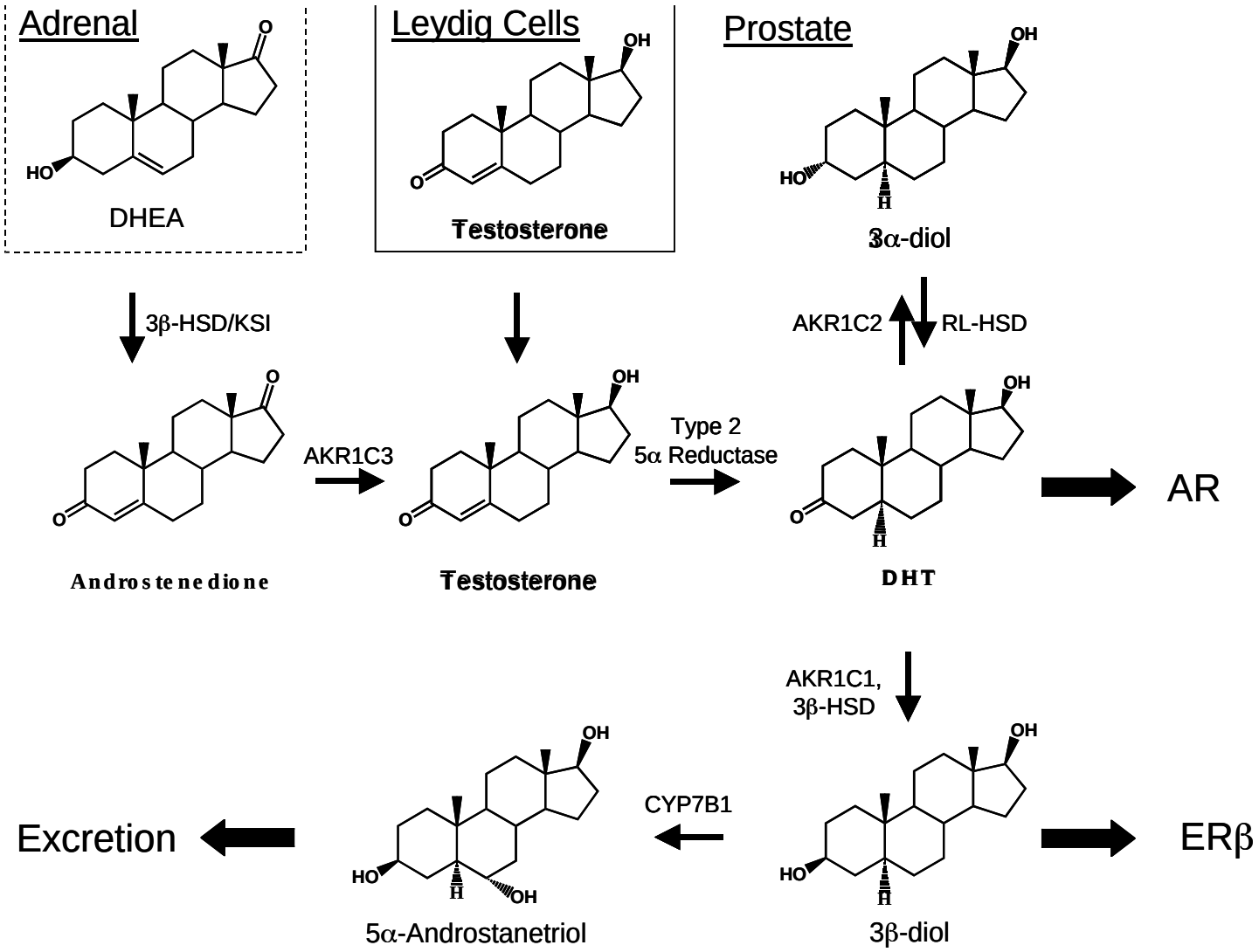
Adrenal
DHEA
Leydig Cells
Testosterone
Prostate
3α-diol
3β-HSD/KSI
AKR1C2
RL-HSD
AKR1C3
Type 2
5α Reductase
AR
Androstenedione
Testosterone
DHT
AKR1C1,
3β-HSD
Excretion
CYP7B1
ERβ
5α-Androstanetriol
3β-diol

Figure 1

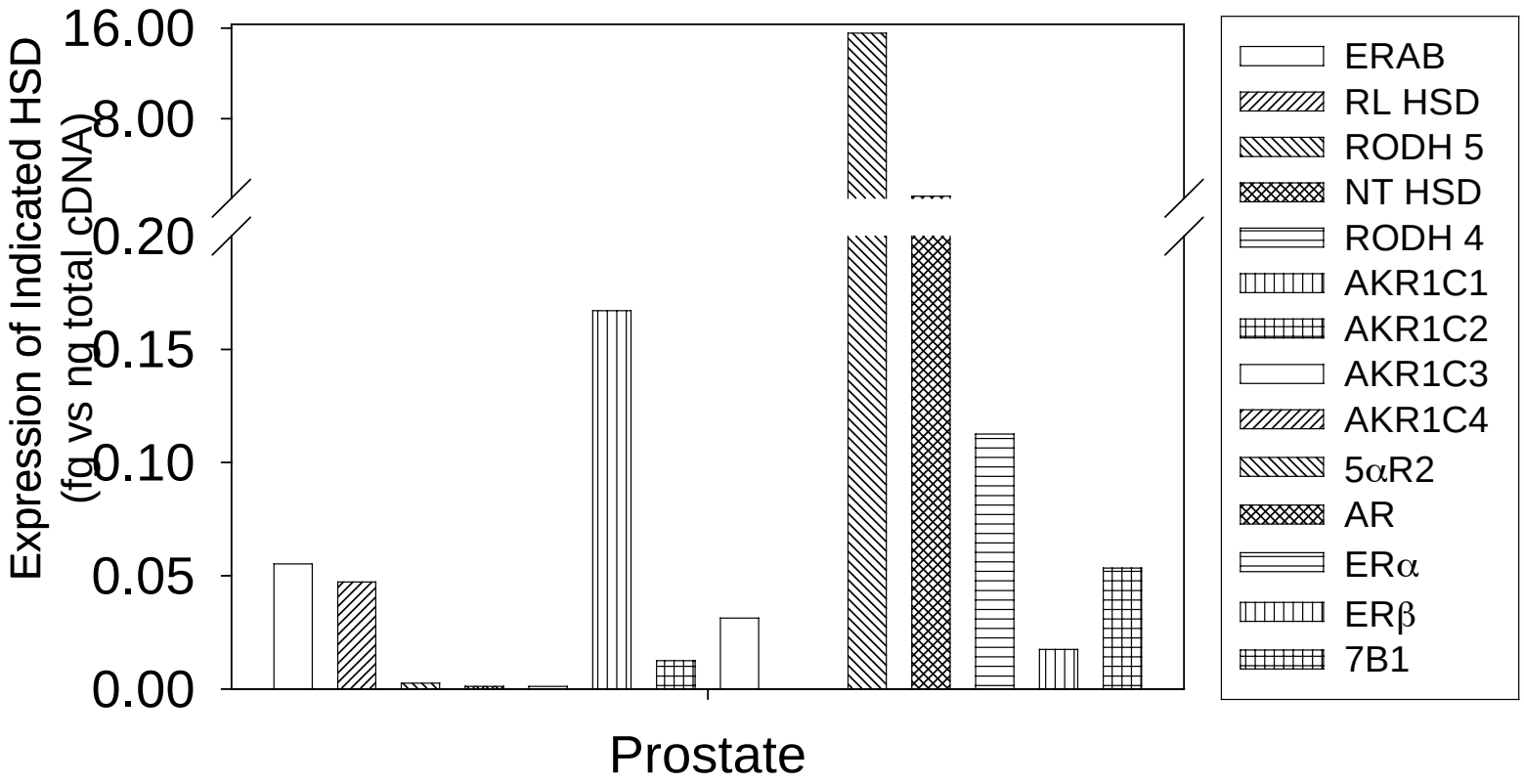
16.00
8.00
0.20
0.15
0.10
0.05
0.00
Expression of Indicated HSD
(fg vs ng total cDNA)
Prostate
ERAB
RL HSD
RODH 5
NT HSD
RODH 4
AKR1C1
AKR1C2
AKR1C3
AKR1C4
5αR2
AR
ERα
ERβ
7B1

Figure 2

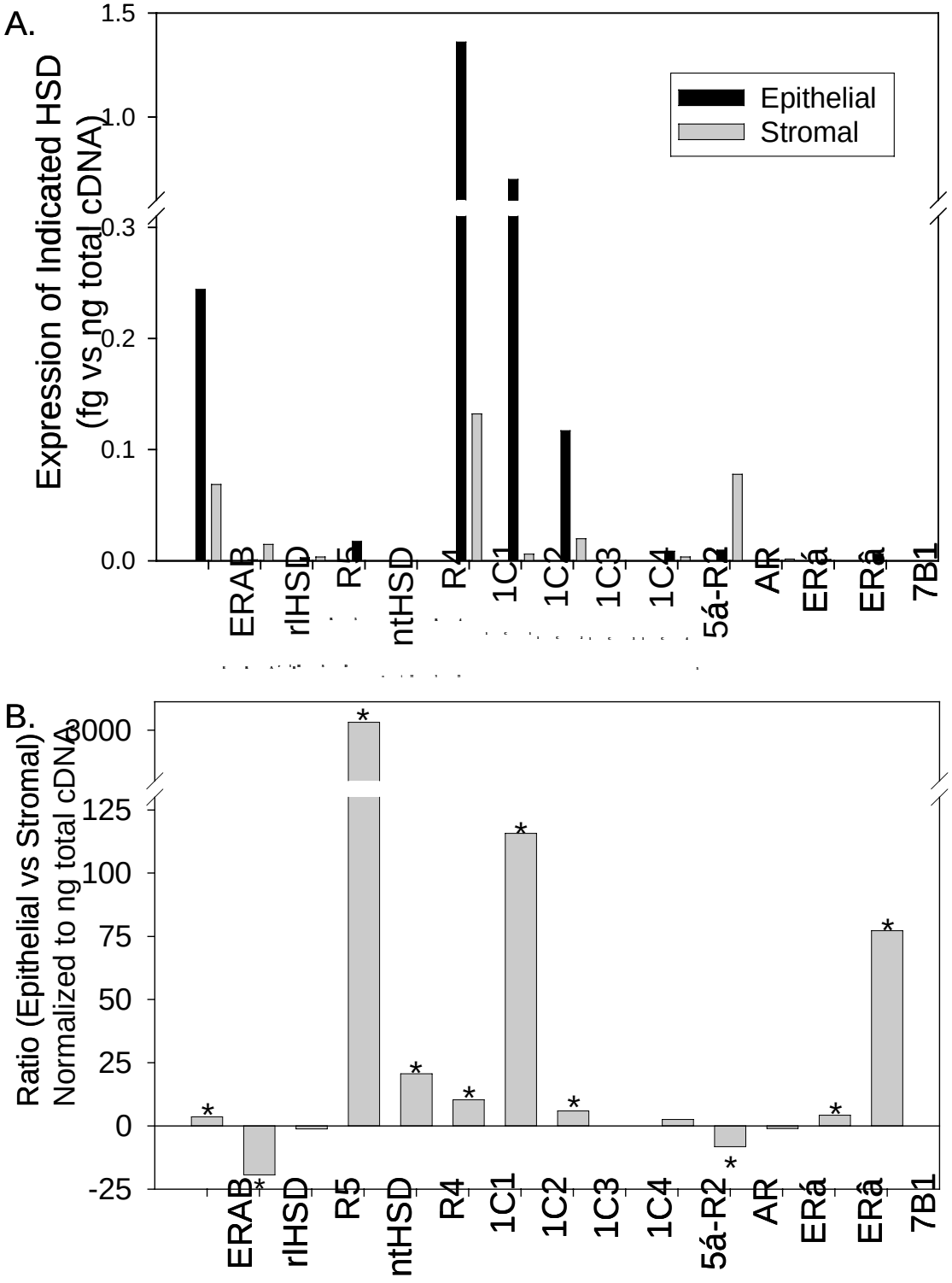
A.
Expression of Indicated HSD
(fg vs ng total cDNA)
1.5
1.0
0.3
0.2
0.1
0.0
Epithelial
Stromal
ERAB
rlHSD
R5
ntHSD
R4
1C1
1C2
1C3
1C4
5á-R2
AR
ERá
ERâ
7B1
B.
Ratio (Epithelial vs Stromal).
Normalized to ng total cDNA
3000
125
100
75
50
25
0
-25
*

Figure 3

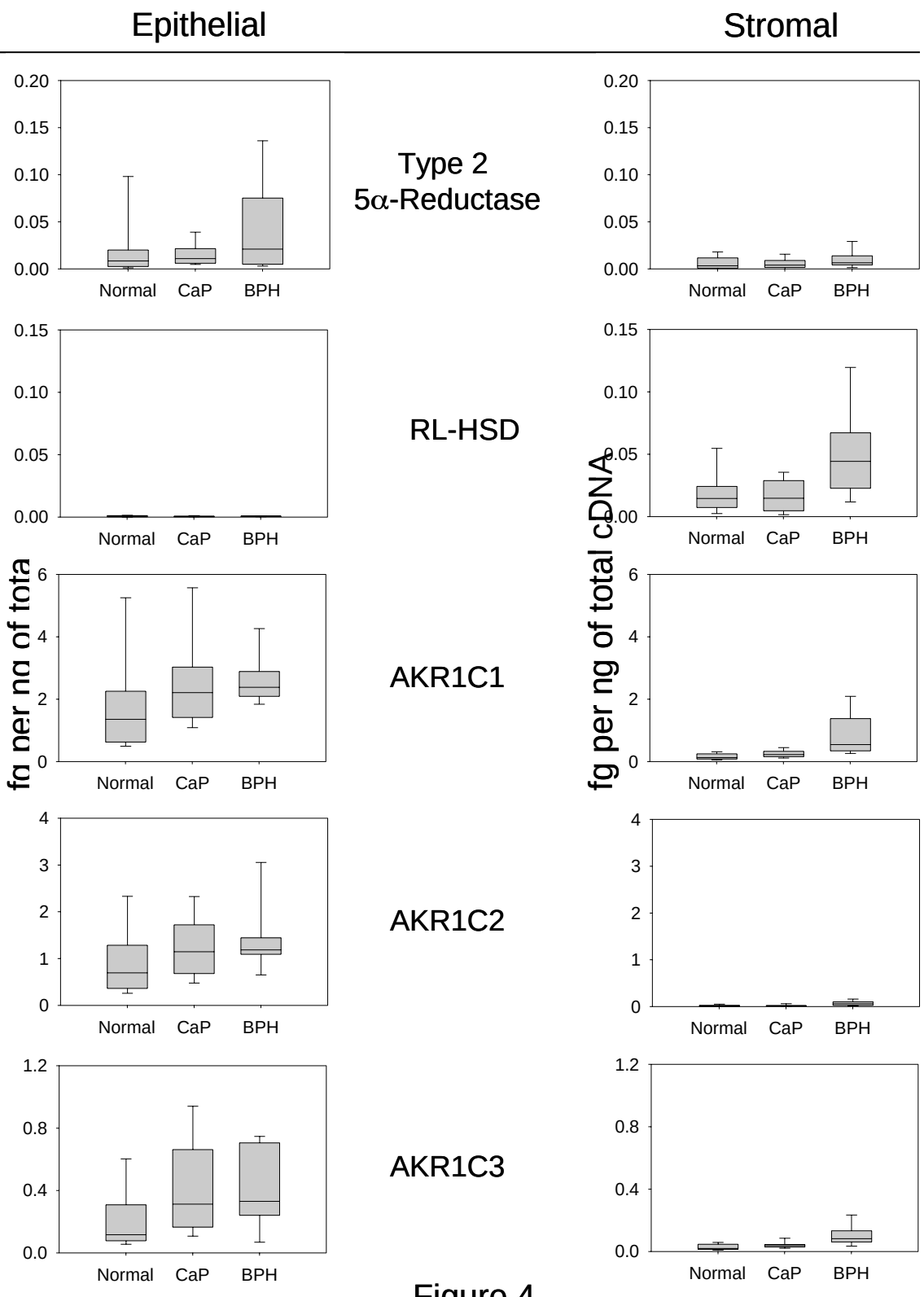
Epithelial
Stromal
Type 2
5α-Reductase
RL-HSD
AKR1C1
AKR1C2
AKR1C3
fg per ng of total cDNA
Normal
CaP
BPH

Figure 4

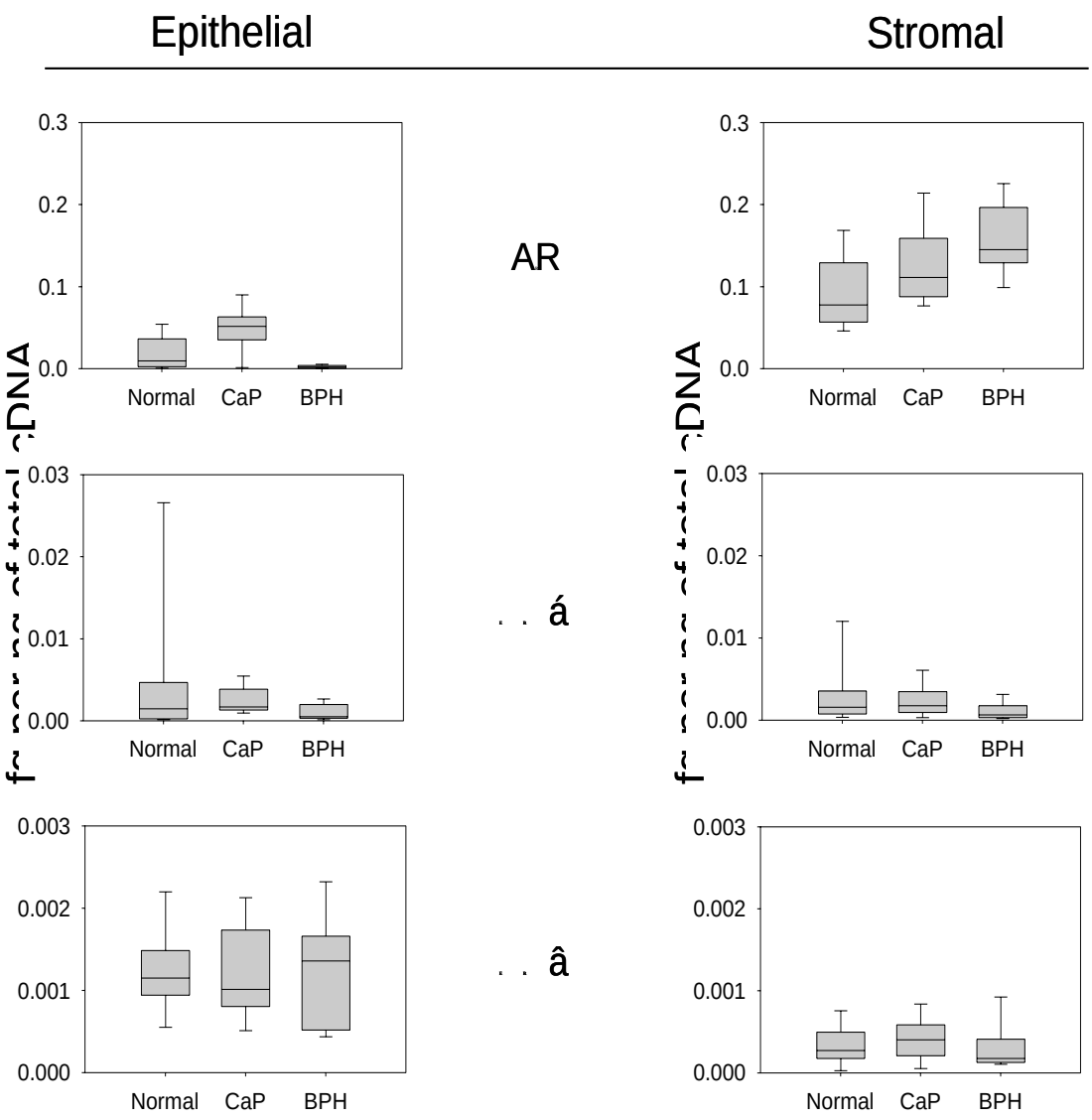
Epithelial
Stromal
AR
0.3
0.2
0.1
0.0
0.03
0.02
0.01
0.00
0.003
0.002
0.001
0.000
Normal
CaP
BPH

Figure 5

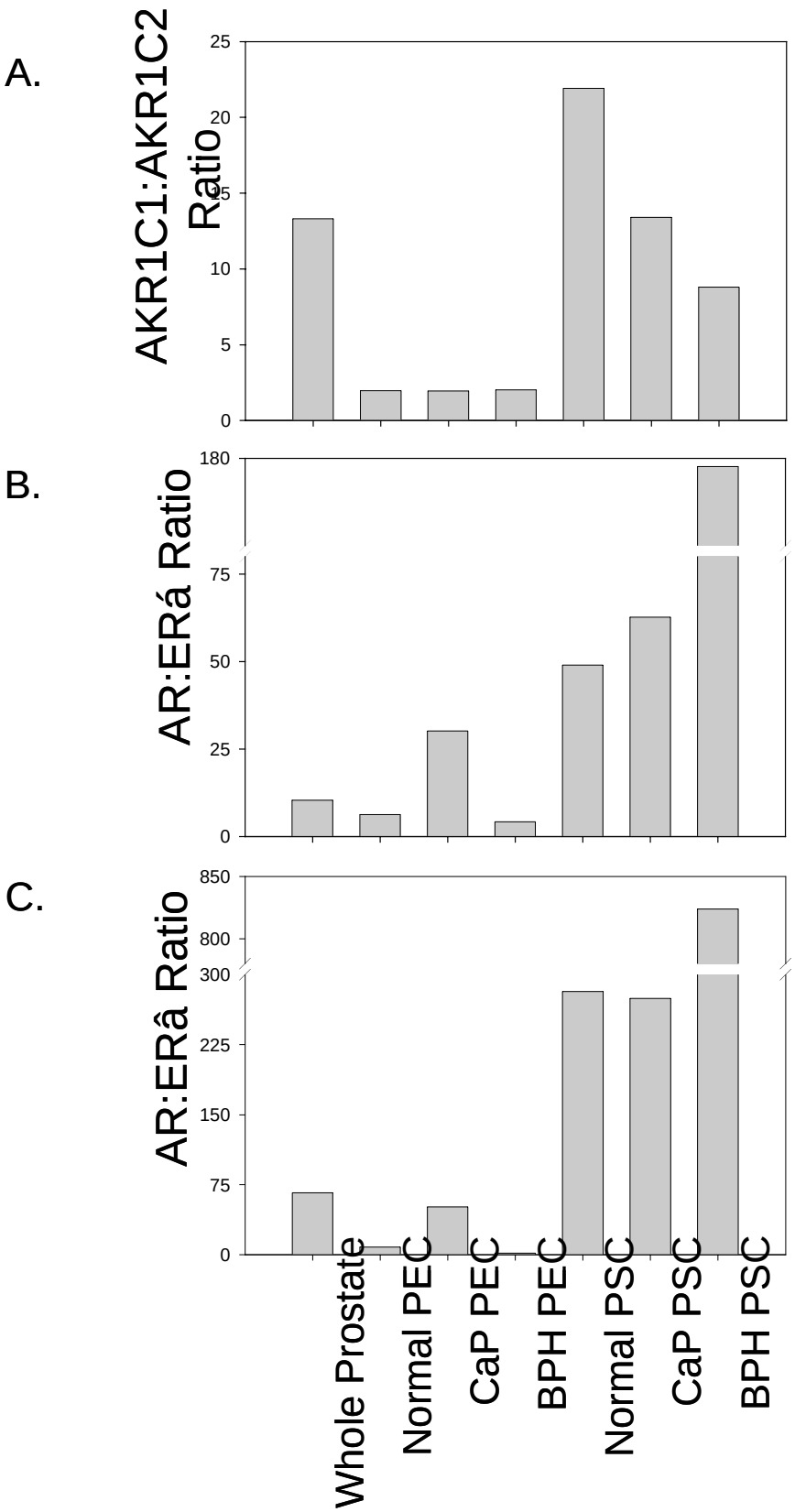
A.
AKR1C1:AKR1C2 Ratio
25
20
15
10
5
0
B.
AR:ERá Ratio
180
75
50
25
0
C.
AR:ERâ Ratio
850
800
300
225
150
75
0
Whole Prostate
Normal PEC
CaP PEC
BPH PEC
Normal PSC
CaP PSC
BPH PSC

Figure 6

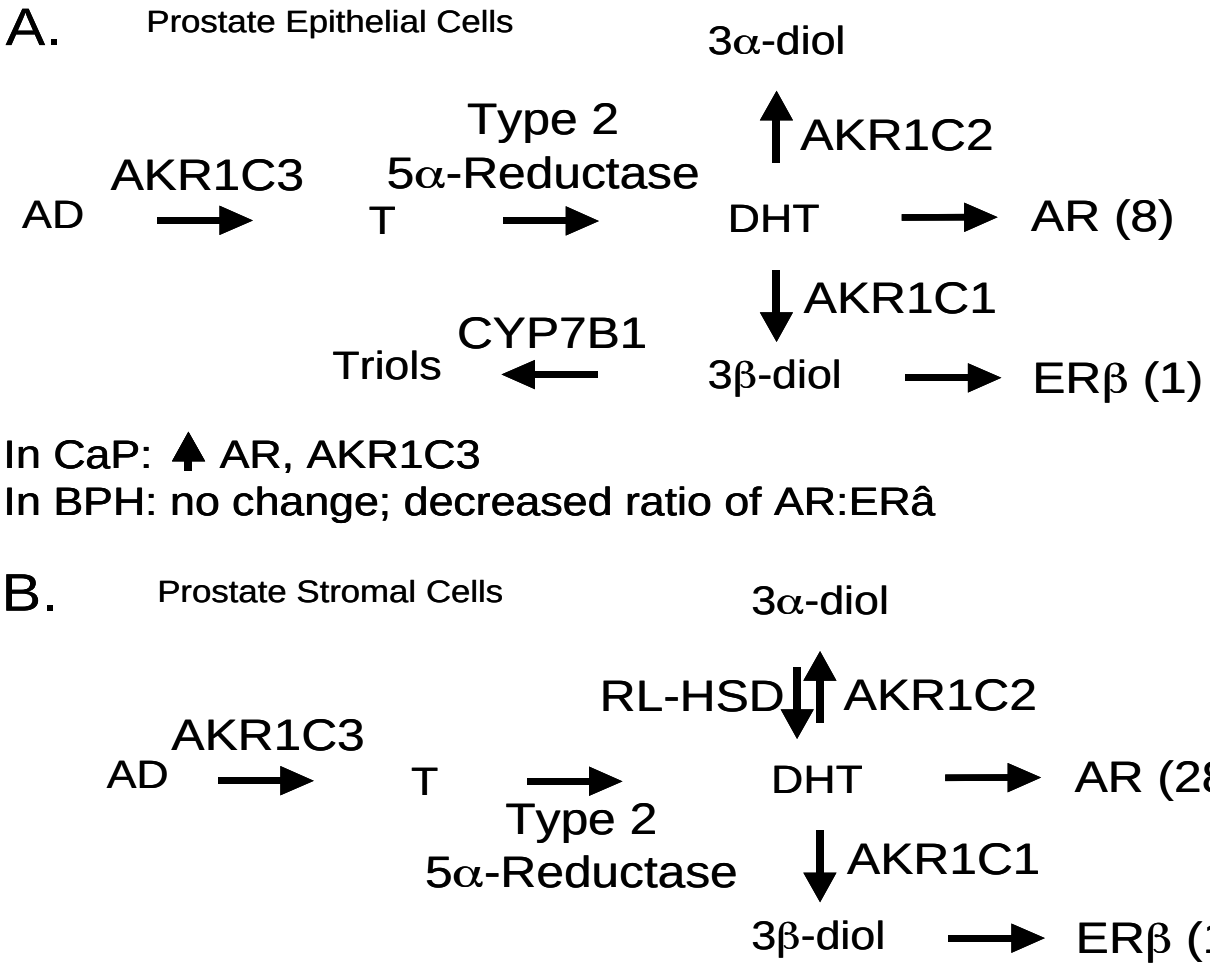
A.
Prostate Epithelial Cells
3α-diol
Type 2
5α-Reductase
AKR1C3
AKR1C2
AD
T
DHT
AR (8)
AKR1C1
CYP7B1
Triols
3β-diol
ERβ (1)
In CaP: ↑ AR, AKR1C3
In BPH: no change; decreased ratio of AR:ERâ
B.
Prostate Stromal Cells
3α-diol
RL-HSD
AKR1C2
AKR1C3
AD
T
DHT
AR (280)
Type 2
5α-Reductase
AKR1C1
3β-diol
ERβ (1)
In CaP: ↑ ERAB, RODH 5, RODH 4, AKR1C1
In BPH: ↑ ERAB, AKR1C1, AKR1C2, AKR1C3, RL-HSD, AR
Increase ratio of AR:ERβ

Figure 7